one PAC that starts with a massive calcarenite bed overlain with a marl and then shallows upward to a soil. The B sequence contains three PACs in which each cycle starts with a calcarenite bed and ends with a soil. The C sequence contains one PAC that consists of a massive calcarenite bed at the base and ends with a moderately-developed paleosol (paleosol D3-5) with horizonation.

Stair Hole

Correlation of the equivalent section at Stair Hole is based on tracing and matching the lower surface of the massive Broken Shell Limestone Member from Durlston Bay. The thickness of the Stair Hole section from the base of the Cinder Member to the base of the Broken Shell Limestone Member is 10 meters compared to 40 meters at Durlston Bay. The upper study interval at Stair Hole is highly condensed and measures only 1.5 meters in thickness (Figure 34). The A sequence is represented by one PAC that has a calcarenite bed at the bottom with a soil on top. The B sequence contains 3 thin PACs. PAC 1 and 2 each consists of a micrite bed with pelecypods and peloids (sample S-4) overlain by a thin shale. PAC 3 consists of a limestone bed, then a marly shale bed, and a soil. Along with the A and B sequences, the C is also very condensed. It consists of one PAC that starts with a sparse biomicrite bed with pelecypods (sample S-3) and then an unsorted biosparite bed with pelecypods (sample S-2) that is overlain with a soil.

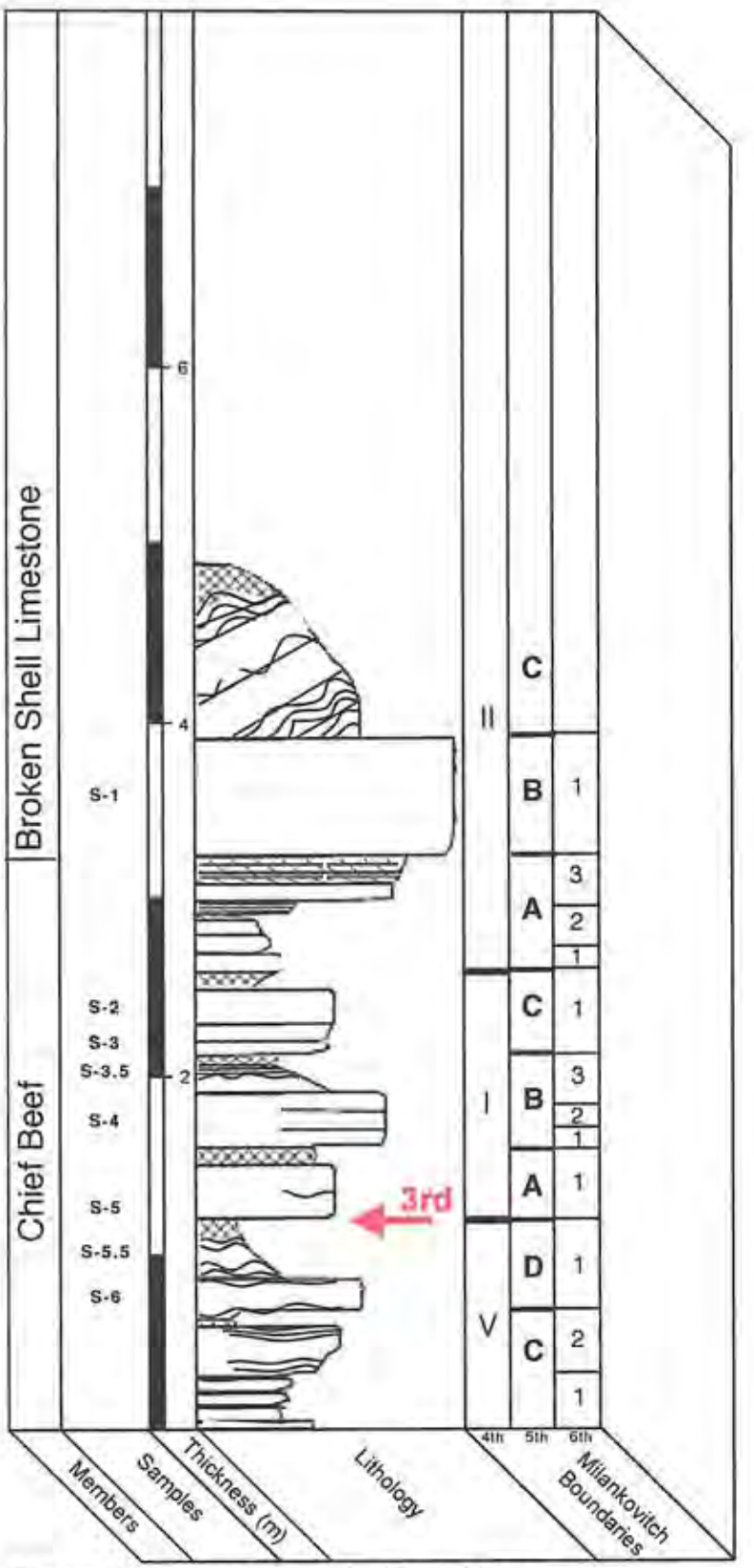

Figure 34. Upper interval at Stair Hole.

CHAPTER 7
ACCOMMODATION SPACE

Variations in thickness of cycles and missing cycles in the Milankovitch hierarchy within the study intervals are best explained by variable development of accommodation space restricting the deposition of shallowing upward sequences. Factors that affect accommodation space are local subsidence rates, eustatic sea-level change, compaction, waves and currents influencing sediment transport and deposition, differential tectonic movements, and the abundance of grains by carbonate-producing organisms (Strasser et al., 1999). The rate of production of accommodation space can cause changes to either deeper or shallower facies. It can also control the amount of sediment or the thickness of sequences that can be preserved. The thickest beds are formed in areas of high accommodation, but only if there is enough carbonate productivity to fill the space available. However, if carbonate productivity was lacking when abundant accommodation space was available, the sequences would not have reached the maximum potential thickness. In areas where there is low accommodation, such as on the landward margin of a shallow carbonate platform, there would be less available space, producing condensed or missing sequences. In particular, precessional cycles (PACs) are missing near the basin margin because sea-level and tectonic subsidence did not produce sufficient accommodation space for sediments to be deposited. However, little or no subsidence could also promote the loss of a 6^{th} order sequences within a larger-scale sequence because during a sea-level fall deposited sediments may be reworked and/or eroded. Evidence within a section that implies reworking and erosion

includes conglomerates at the top of a cycle with pebbles of different lithology than in the underlying sequence (Strasser et al., 1999)

Missing cycles occur in sediments and sequences deposited near the basin margin, whereas in deposits more basinward, increased accommodation space results in thicker and more complete sections. In other words, cycles located near the basin margin and at topographic highs tend to be thinner and less complete. Goldhammer et al. (1990, 1993) explain this by inadequate accommodation near the basin margin resulting in partial deposition or less preservation of deposited sediments during major sea-level fluctuations. Pasquier and Strasser (1997) observe in their research that in the French Jura there are fewer elementary sequences preserved in platform margin facies than in more basinal facies. In addition, Strasser et al. (1999) observed that elementary and/or small-scale sequences can be condensed or missing when close to the basin margin because there is a lower accommodation potential there than within the basin. In the French Jura, up to one elementary sequence (PAC) is observed in the small-scale sequences of Strasser (i.e. 5^{th} order sequences) when accommodation is low and up to six elementary sequences when accommodation rates are high. These observations can also be seen in the columns drafted for my study. The most complete section (type section) at Salève is interpreted to have been deposited more basinward where accommodation rates were higher. Whereas, sections at Crozet, Chapeau de Gendarme, and Yenne show missing cycles that suggest they were deposited closer to the basin margin where accommodation rates were lower. The Dorset coast shows one of most extreme examples of lateral variation in addition to decreased accommodation space where it is lowest at the basin margin and significantly higher more basinward. Deposits at Dulrston Bay (the

type section for the Purbeck) show a complete hierarchic stacking pattern, whereas cycles in basin margin deposits at Stair Hole are 1/4 the thickness and are missing most of the 6^{th} order sequences. Anderson (2001 b) also observed this same trend in his research on the Dorset coast, and states that sections (like Durlston Bay) located more basinward where the subsidence rate or accommodation space is greater will contain thicker cycles and more complete sections.

CHAPTER 8
PALEOSOLS

Cycles and sequence boundaries in the French Jura and the Dorset coast are often characterized by paleosols. Paleosols found below cycle boundaries suggest that a more extreme sea-level event occurred, such as those that occur at 3rd, 4th, or 5th order boundaries in the Croll-Milankovitch model (Francis, 1986; Wright, 1994; Wright, 1996). According to the Croll-Milankovitch model there may be short intervals (20 to 100 ka) of exposure or erosion between sea-level flooding events that cause soils to develop during lowstands. Therefore, the development of paleosols within my study intervals should be slight and should only have had enough time to develop Entisols or Inceptisols (Retallack, 1997; Birkland, 1999). Entisols are poorly developed (i.e., a soil profile with A and C horizons) and are classified in this order when the soil profile does not meet the criteria of any other soil order. Whereas, Inceptisols show pedogenic features that indicate a more developed soil than Entisols and contains a diagnostic horizons (i.e., a soil profile with A, B, and C horizons). Paleosols previously identified below cycle boundaries in my study areas have the following characteristics: in place root structures, orange strata, laminated horizons, massive horizons, brecciated horizons, burrows, and peds (Seier and Anderson, 2002).

Palaeopedology methods are most useful in combination to form interpretations about the past history of paleosols. These include field observations, thin section analysis, chemical weathering ratios, and X-ray diffraction for clays. Macroscopic pedogenic features described in the field included those described by Wright (1994). Thin section analysis involved microscopic identification of soil fabrics, mineralogy, and

pedogenic features. Molecular weathering ratios provide information on the relative degree of soil development, paleoenvironment, and ancient soil processes. X-ray diffraction was used to identify clays (not translocated) in each sample. All techniques were attempted on each paleosol sample. Most samples show few pedogenic features, which could indicate that over the last 140 Ma the soil structure and chemistry has been overprinted or destroyed. This is not surprising since these rocks and soils in study have been buried, uplifted, and physically and chemically altered.

Molecular Weathering Ratios

There are six variables based on molecular weathering ratios that are used to evaluate or characterize soil development and maturity; they include hydration, salinization, oxidation, hydrolysis, leaching, and calcification. Molecular weathering ratios are calculated from oxide weight percents determined by ICP-MS. (Appendix C). Oxide weight percents are derived from raw ICP data that is in the form of element weight percent (Appendix C). Techniques in calculating and interpreting these ratios follow that of Retallack (1990, 1997) and Birkland (1999). The error in the value in each data point from ICP analysis is at most 10%, and therefore the maximum error of any data point is around 0.14. In my data, this error is not significant, and if error bars were put on the molecular weathering ratio profile they would appear as big as the plotted data points.

Geochemical trends in molecular weathering ratios profiles that are not pedogenic in origin result from parent material consisting of a shallowing upward facies. Each paleosol appears near the top of a cycle that shows shallowing upward facies. Samples

taken from the bottom of most paleosol profiles were rich in carbonate, and samples taken near the top are more shale. These shallowing upward facies also have a geochemical trend that shows more Ca and Mg at the bottom of each profile, and more Si and Al toward the top. This geochemical trend that is not pedogenic in origin is taken into consideration when making interpretations for molecular weathering ratios.

Hydration

Hydration can be represented by silica divided by alumina (SiO_2/Al_2O_3). Both silica and alumina are constituents of layer-lattice silicate minerals. This ratio mainly reflects clay content (Feakes and Retallack, 1988). The increase in the amount of clay minerals in a profile will result in decreasing values of this ratio.

Salinization

The ratio that defines salinization is the total amount of soda over potash (Na_2O/K_2O). When this ratio is equal to or greater than 1, there is a high degree of salinization (Na) within the profile (Retallack, 1990). Porous soil, in combination with increased amounts of precipitation, allows the soil to be well-drained and remove away more soluble (mobile) ions (Na). Under the same conditions, potassium is not as soluble and will not be stripped away as quickly. Therefore, under such conditions ratios will be very low and indicate that salinization is not a significant factor on the history of this soil. Salinization can also be represented by alkalies over aluminia $(Na_2O+K_2O)/Al_2O_3$. The accumulation of clays within a profile will decrease this ratio.

Oxidation

The relationship of reduced and oxidized iron to clay content is represented by the ratio of total iron (expressed as Fe_2O_3) divided by alumina (Fe_2O_3/Al_2O_3) (Retallack, 1990). This ratio will decrease in areas where clays are present. Most soils show values of 0.4 or less (Marbut, 1935). Ratios may increase to values of 1.9 in highly oxidized soils (Retallack, 1997).

Hydrolysis

The degree of hydrolysis can be represented as bases over alumina ($Na_2O+MgO+K_2O+CaO/Al_2O_3$). This ratio can be used as an indication of pH and the development of the soil (Retallack, 1990). Ratios greater than 1 indicate that the soil is very basic and/or is weakly developed. For well-developed soils, carbonic acid reacts with cations (bases) to form clays, and the soil tends to be more acidic and have ratios less than 1. Increased values within a profile reflect accumulation of bases in certain horizons, such as the presence of a calcic horizon (Bk).

Leaching

The solubility differences of barium and strontium make this ratio (Ba/Sr) an indication for the amount of time the soil developed and/or the degree of leaching (Birkeland, 1999; Retallack, 1990). In minerals, barium is much less soluble than strontium. Therefore, in a well-drained soil or one that has formed over a long period of time, Ba is less leached than Sr within the profile. Soils that are strongly leached usually have a ratio around 10. However, most soils show ratios of around 2.

Calcification

Relative degrees in calcification, $(MgO+CaO)/Al_2O_3$, indicate pH and also the presence of calcic horizons and/or nodules. Soils with ratios less than 2 indicate more acidic soils. Soils with ratios that range from 2-10 indicate calcic soils. Ratios equal to or greater than 10 indicate a calcic soil with possible calcic horizons and/or nodules.

Trace Elements

Trace elements plotted alone with depth can suggest the presence of clays and/or organics within the profile (Retallack, 1997). The trace elements used in this study include Zn, Ni, Cu, and Cr. Trace elements tend to show increasing concentrations with the presence of clays and/or organics. However, increases in trace elements cannot determine if clays have been translocated.

X-Ray Diffraction

X-ray diffraction (XRD) is used for the identification of clays in a sample (Retallack, 1997). The sample is exposed to X-rays at different angles, and the intensity of the reflection is presented on a diffractogram. The inter-layer lattice spacing of a specific clay causes the reflection of the X-rays. Each clay has a different pattern on the diffractogram. More intense X-rays reflected from lattice spacings within a clay causes peaks, and multiple peaks are spaced from one another at certain degrees (2 Theta). These spacing characteristics allow for the identification of specific clays (kaolinite, illite, or smectite) and other minerals commonly found in paleosols (calcite and quartz).

This method can not determine the origin of the clay, such as diagenetic, detrital, or pedogenic.

Paleosol Classification

Paleosols were classified using the United States Department of Agriculture (USDA) soil taxonomy (1998) and Mack et al. (1993). The USDA classification is widely used for modern soils. The problems that arise in paleosols are not taken into consideration and much interpretation is needed for such detailed subdivisions (Retallack, 1983). The identification of the taxonomic class of a soil consists of the order, suborder, great group, and subgroup. The Mack et al. (1993) classification uses descriptive pedogenic features that have a high preservation potential in the rock record. This classification uses easily recognizable macro- and microscopic morphological and mineralogical features. The identification of the class of a soil consists of the order and a subordinant modifier when needed. Both classification schemes will be used to classify each paleosol.

Paleosols in the French Jura and the Dorset Coast

The investigation of paleosols within the study interval includes two in the French Jura and two in the Dorset coast. The paleosols sampled in the French Jura include one sampled from the upper interval at Salève (sample S-19, Figure 27) and another from the lower interval at Cozet (sample R-2, Figure 25). In Dorset one was chosen from the lower interval at Durlston Bay South (sample D1-6, Figure 31) and another from the upper interval at Durlston Bay North (sample D3-5, Figure 33). The paleosols in study

were chosen because of there distinct macroscopic features in outcrop that included 30 cm or more thickness of unlithified sediment below major (4^{th} order) sequence boundaries, color differentiation and horizonation within the profile, the presence of organic material and or peds near the uppermost parts of the profile, and the presence of relict bedding near the base of the profile.

The paleosols in study are interpreted to have developed during similar climate, and have similar topography and parent material. Paleosols within my study intervals developed in conditions that were warm and humid during the Berriasian (Allen, 1998). Most likely, these profiles developed under monsoonal wet-dry conditions (classification from Retallack, 1997). These paleosols formed very close to the sea, and the paleotopography can probably be described as a moderately-drained lowland (classification from Retallack, 1997). However, more developed paleosols (D1-6 and D3-5) that contain one or more of certain distinguishing horizons and clays (illite, smectite, and kaolinite) could indicate more precipitation during formation or a well-drained profile that was located further from the sea. In addition, the porosity of the parent material can also control the drainage of a soil. The parent material for these paleosols consists of fossiliferous micrite with the possibility of calcite cement between grains. These paleosols were formed on a carbonate platform of shallow peritidal sediments. The parent material may vary in porosity depending on the amount of calcite cement that fills spaces between carbonate grains and/or the amount of larger fossils present in the sediment. However, little spar or fossils were detected in thin section. Alteration of these features is likely during diagenesis and soil development through the reaction with carbonic acid during pedogenesis.

Thin section analyses reveal a lack of original organics or minerals that formed in place during paleosol development. In situ roots were not detected micro- or macroscopically, and plant material that was found in these profiles is considered strictly detrital. However, if organic material at one time was present, it might have been consumed by organisms within the past 140 Ma. Thin section analysis also detected hematite, pyrite, and euhedral gypsum scattered throughout the profiles. The occurrence of these minerals is interpreted as diagenetic. The formation of gypsum ($CaSO_4$) and hematite (Fe_2O_3) during diagenesis was probably formed by the reaction with calcite ($CaCO_3$) and pyrite (FeS_2).

The time interval over which pedogenesis occurred is difficult to interpret because very few soil features were present, and it is likely that the chemical signatures have been altered slightly due to diagenetic recrystallization. In determining the time for development, all palaeopedology methods are taken into consideration. The lack of pedogenic features within these paleosols prevents a more in depth characterization in interpreting their history and time of development. However, most profiles show a weakly to moderately developed A horizon, which Birkeland (1999, p. 225) states can be achieved within 100 to 5000 years.

CROZET (R-2)

Analysis

The R-2 profile at Crozet is weakly developed. It shows a poorly developed A horizon and relict bedding in the C1 and C2 horizons (Table 1 & Appendix A). The horizons

Table 1. Crozet paleosol profile (R-2)

Horizon	Description
A	(0-10 cm) Fresh (Gley 1 8/5G light greenish grey); organic rich lime mud; Reacts with HCl; Macro: relict bedding, organic rich pebbles; Micro: peat, carbonized plant fragments.
C1	(10-80 cm) Fresh (Gley 1 8/N white); lime mud; Reacts with HCl; Macro: relict bedding; Micro: hematite, pyrite, quartz, fine grained dolomite, foraminifera; XRD: calcite.
C2	(80-150 cm) Fresh (Gley 1 8/N white); lime mud; Reacts with HCl; Macro: relict bedding; Micro: hematite, pyrite, quartz, fine grained dolomite.

show distinct color changes from light greenish grey to white. Thin section analyses reveal an abundance of organics in the A horizon, and diagenetic hematite, pyrite, and quartz in the C1 and C2 horizons (Table 1). The A horizon is characterized by organic rich pebbles, peat, and plant fragments in thin section. Molecular weathering ratios further support the presence of organics in the A horizon, as indicated by the increase in values of the Zn, Ni, and Cr trace elements (Figure 35 & Appendix C). These trace elements form complexes with organics found in the A horizon. Higher leaching values indicate the A horizon was well-drained and not water logged. Leaching values in the A horizon are of normal soils and the C1 and C2 horizons show significantly lower values that can indicate poor drainage. The oxidation values are of normal soils in the C1 and

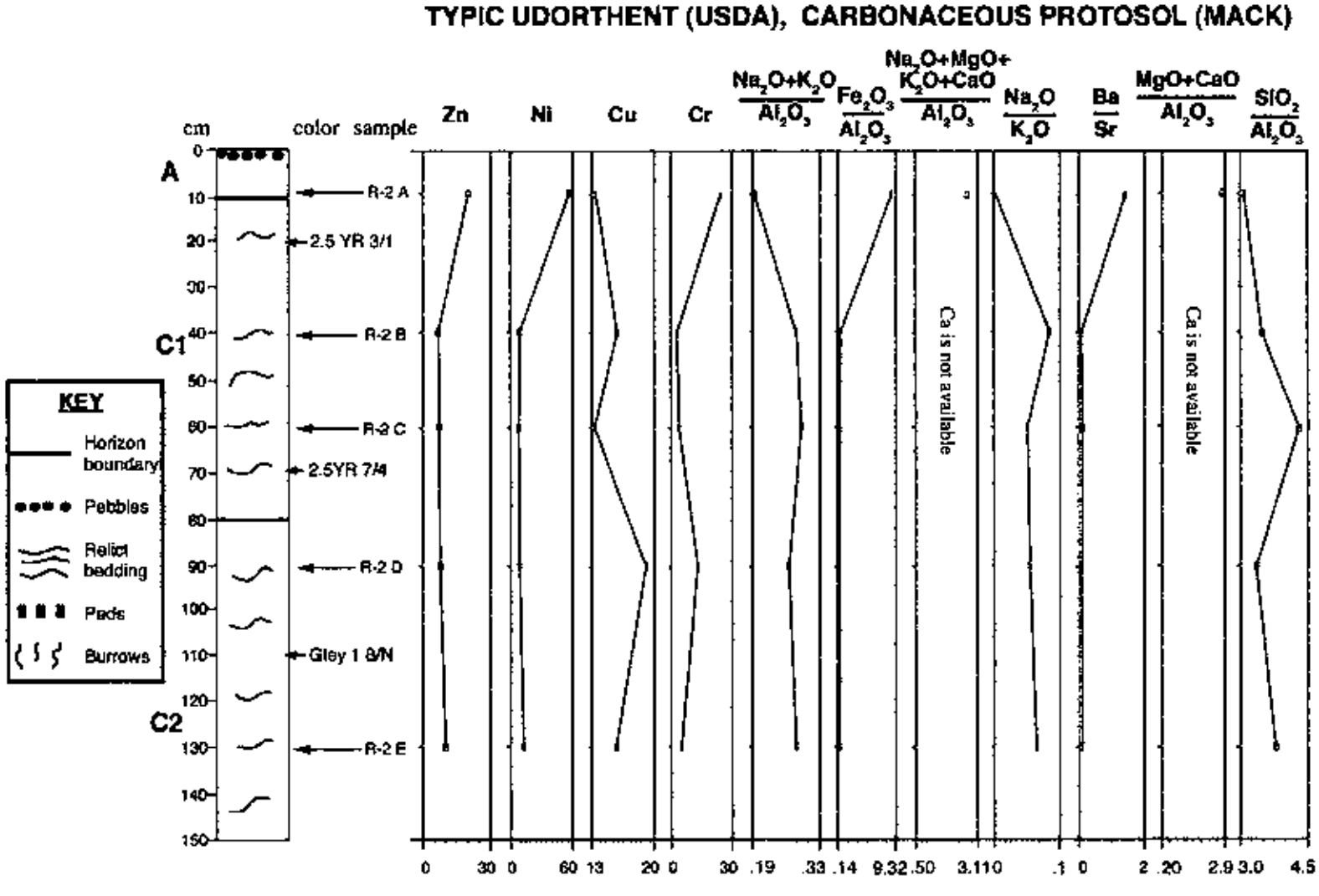

Figure 35. Molecular weathering ratios at Crozet (R-2).

C2 horizons, but show an increase in the A horizon. The hydration ratio indicates the presence of clay or organics in the A horizon and in the top of the C2 horizon. The salinization ratio $(Na_2O+K_2O)/Al_2O_3$ shows a decrease in the A horizon, but this does not indicate clays because there are decreased values of Na_2O in this horizon. This decrease of Na_2O can be seen in the decreased salinization ratio Na_2O/K_2O. The presence of clays is not recognized in thin section, and XRD analysis indicate that illite, smectite, and kaolinite is absent throughout the profile (Figure 36).

Classification

I classify this soil as a Typic Udorthent under USDA standards. The taxonomic class is interpreted as an Entisol. This soil does not show any distinguishing features that would allow for a more descriptive name. Therefore the suborder, great group, and subgroup is classified, according to the name, as a soil that has other or no distinguishing characteristics to allow classification to a more descriptive subdivision.

This paleosol is classified as a Carbonaceous Protosol under Mack et al. (1993) standards. I feel that this name better describes this soil than the one above. This soil is named for its weak development and poorly developed features. The subordinate modifier (Carbonaceous) is used to describe the A horizon having an abundance of peat and organic rich material.

KEY

I = Illite
S = Smectite
K = Kaolinite
Q = Quartz
C = Calcite

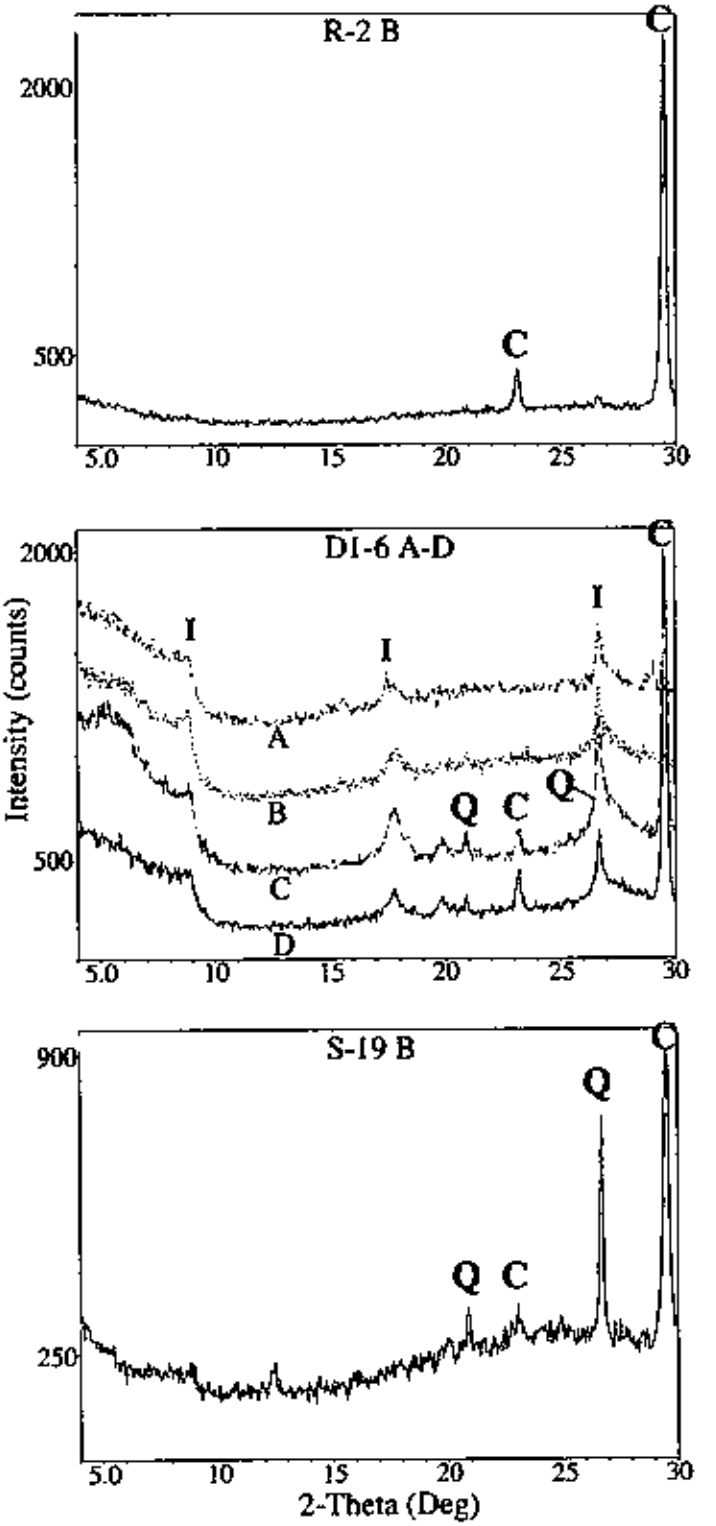

Figure 36. X-ray diffraction of samples R-2 B, D1-6 A-D, and S-19 B.

DURLSTON BAY (D1-6)

Analysis

The profile D1-6 at Durlston Bay (South) is moderately developed with blocky peds in the A horizon and relict bedding in the Bw2 and C horizons (Table 2 & Figure 37). Each horizon shows a distinct color change, aside from the Bw2 horizon that is similar in color to the Bw1 horizon, but contains relict bedding. Thin section analyses reveal an abundance of diagenetic minerals and detrital plant fragments throughout the profile (Table 2). XRD analyses indicate that illite is also present throughout the profile (Figure 38). The XRD data show distinctive illite peaks at 8.8°, 17.7°, and 26.6° (2theta). Calcite and quartz is also present in samples B, C, and D. Calcite shows peaks at 23° and 29.3°, and the peaks for quartz are at 20.8° and 26.6° (2Theta). The molecular weathering ratios for this profile further indicate characteristics that distinguish the horizons (Figure 38). The A horizon shows more plant fragments than in the other horizons, which may explain the increases of Cu toward the top of the profile in the A horizon. The hydration, salinization ($(Na_2O+K_2O)/Al_2O_3$), and oxidation ratios indicate an increase in detrital clay (Al_2O_3) downward through the profile with a distinct increase in the C horizon at 80 cm. In addition, the trace elements Ni and Cr are consistent with this idea and show increasing trends downward through the profile. Zn shows a distinct spike in the Bw1 horizon. The hydrolysis and calcification molecular weathering ratios also show this distinct increase when comparing the C and Bw2 horizons to the Bw1. This may indicate that the Bw1 is relatively different than the other horizons because it shows an accumulation of bases. Leaching and salinization ratios suggest less than normal values

Table 2. Durlston Bay paleosol profile (D1-6)

Horizon	Description
A	(0-55 cm) Fresh (Gley 1 8/5G light greenish grey); organic rich lime mud; Reacts with HCL; Macro: blocky peds; Micro: carbonized plant fragments (cellular structure), presence of clay (detrital), hematite, pyrite, quartz, dolomite; XRD: illite, quartz, calcite.
Bw1	(55-68 cm) Fresh (2.5 YR 7/2 pale red); organic rich lime mud; Reacts with HCL; Micro: carbonized plant fragments (cellular structure), presence of clay, hematite, pyrite, quartz, dolomite; XRD: illite, quartz, calcite.
Bw2	(68-80 cm) Fresh (2.5 YR 7/2 pale red); organic rich lime mud; Reacts with HCL; Macro: relict bedding; Micro: carbonized plant fragments (cellular structure), presence of clay (detrital), hematite, pyrite, quartz, dolomite; XRD: illite.
C	(80-100 cm) Fresh (2.5 YR 6/3 light reddish brown); organic rich lime mud; Reacts with HCL; Macro: Relict bedding; Micro: carbonized plant fragments (cellular structure), presence of clay (detrital), hematite, pyrite, quartz, dolomite; XRD: illite.

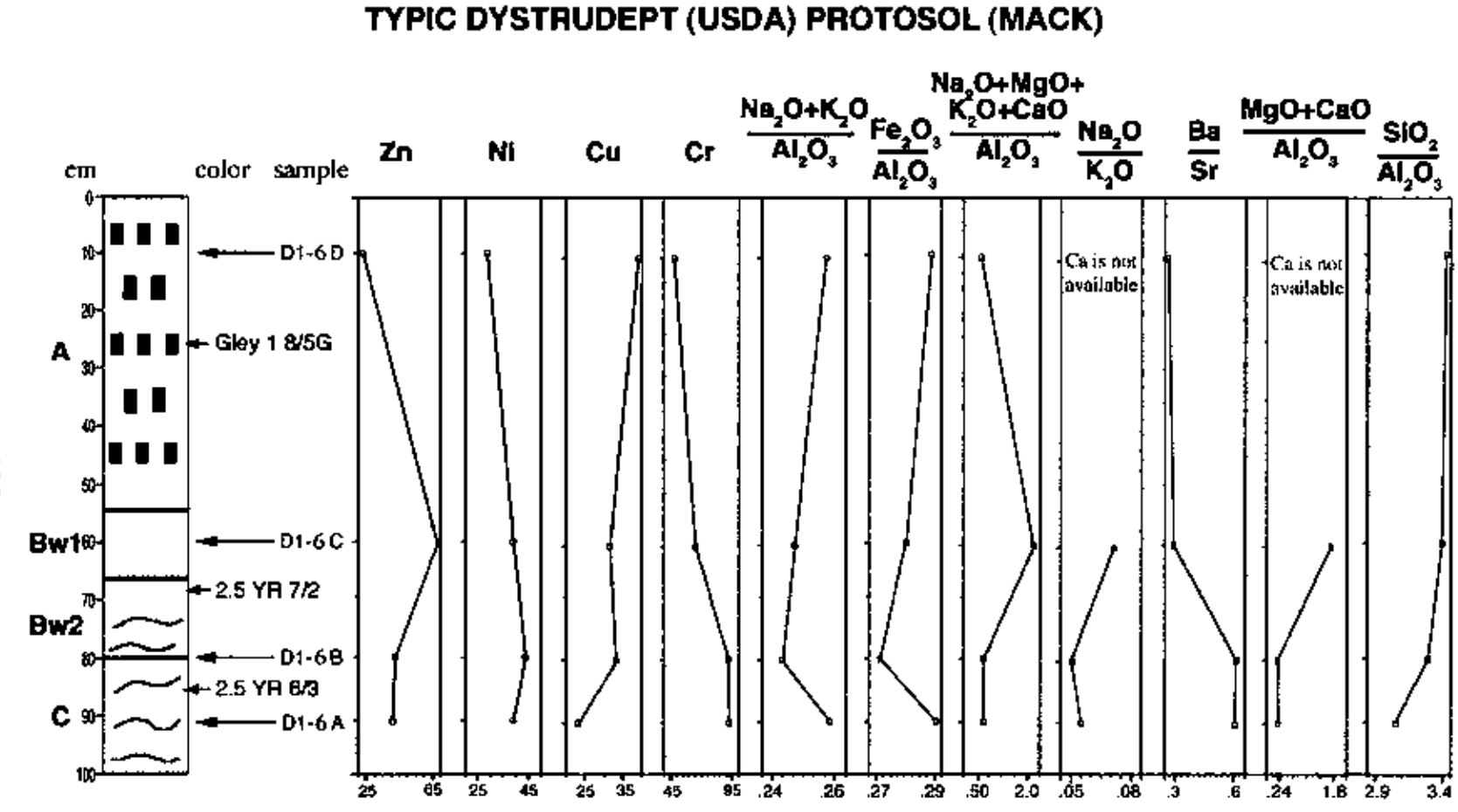

Figure 37. Molecular weathering ratios at Durlston Bay (D1-6).

when compared to most soils. This may suggest a profile that is less leached and/or less developed.

Classification

I classify this soil as a Typic Dystrudept using the USDA classification. The taxonomic class is interpreted as an Inceptisol. This is based on ped structures in the A horizon and the presence of two different B horizons that could indicate more development than in Entisols. The Suborder indicates that development occurred in an udic moisture regime, indicating humid climates that have well distributed rainfall. The great group and subgroup indicate that there are no other distinguishing features that allow for a more descriptive subdivision.

This soil is classified as a Protosol using the Mack et al. (1993) classification. The order is named for its weak development and pedogenic features that are too poorly developed to be the most prominent feature. Subordinate modifiers are not used due to the lack of prominent features. I think that this classification is as descriptive as the USDA classification.

DURLSTON BAY (D3-5)

Analysis

The profile D3-5 at Durlston Bay (South) is moderately developed. This soil contains very few macroscopic features, except for relict bedding in the C horizon (Table 3, Figure 38). Thin section analyses reveal detrital plant fragments, the presence of clay, pelecypods, and diagenetic minerals such as dolomite, gypsum, pyrite, and hematite.

Table 3. Durlston Bay paleosol profile (D3-5)

Horizon	Description
A	(0-25 cm) Fresh (2.5 YR 8/1 white); organic rich lime mud; Reacts with HCL; Micro: carbonized plant fragment, presence of clay (detrital), quartz, dolomite, euhedral gypsum, pelecypods.
Bw1	(25-55 cm) Fresh (2.5 YR 8/4 pink); organic rich lime mud; Reacts with HCL; Micro: carbonized plant fragments, presence of clay (detrital), hematite, pyrite, quartz, dolomite, euhedral gypsum, shells; XRD: illite, quartz, calcite.
Bw2	(55-80 cm) Fresh (2.5 YR 5/2 weak red); organic rich lime mud; Reacts with HCL; Macro: relict bedding; Micro: carbonized plant fragments, presence of clay, shells, hematite, pyrite, quartz, dolomite, euhedral gypsum; XRD: illite, smectite, kaolinite, mixed-layer illite/smectite, quartz.
C	(80-100 cm) Fresh (2.5 YR 6/2 pale red); lime mud; Reacts with HCl; Macro: relict bedding.

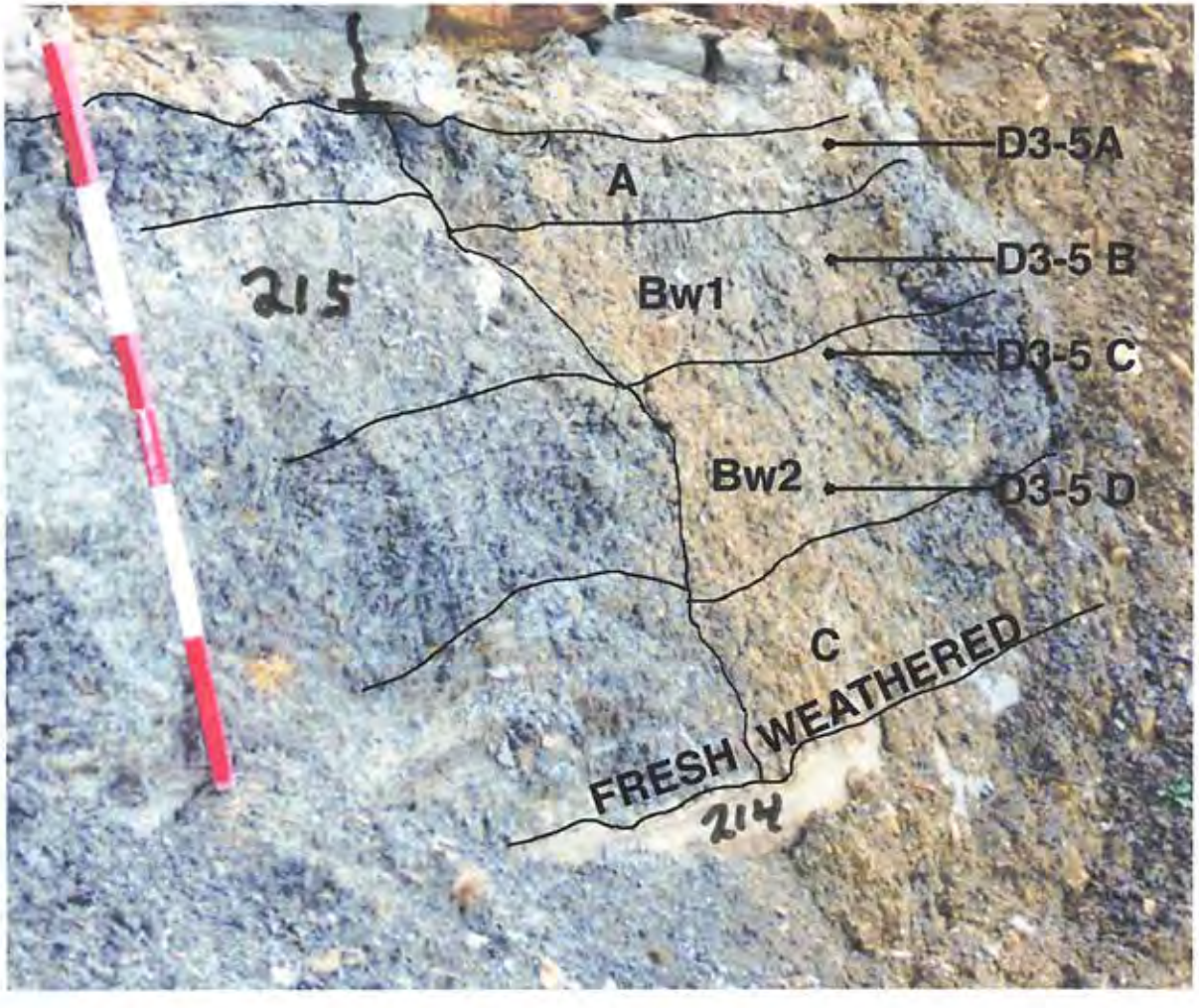

Figure 38. Picture of the D3-5 paleosol profile at Durlston Bay.

The XRD patterns for samples D3-5 B in the Bw1 horizon show characteristic peaks for illite at 8.8°, 17.7° and 26.6° (2theta), and peaks for calcite and quartz (Figure 39). The diffractograms for samples D3-5 C and D in the Bw 2 horizon show peaks for illite/smectite mixed layer, illite, and kaolinite at 6°, 8.8°, 12.2°, 17.7°, 24.8°, and 26.6° (2theta). Glycolation caused the mixed-layered illite/smectite peak at 6° to shift, the 17.7° peak to decrease, and the 26.6° peak to appear. Glycolation did not affect the kaolinite peaks at 12.2° and 24.8°. Upon heating to 550°C, the mixed-layered illite/smectite and kaolinite peaks collapsed to the illite pattern. Quartz is also found in sample D3-5 D.

Molecular weathering ratios are seen in Figure 40. Cu and Cr show increases near the top of the profile in the A horizon, possibly due to increased organics. The most distinctive increase in molecular weathering ratios are in the Bw1 horizon. The distinct increases in the calcification and hydrolysis ratios may suggest an area where bases accumulated. The trace element Zn also shows a significant increase at the Bw1 horizon possibly due to increased bases. The increase of the oxidation ratio at this horizon shows a decrease in clay content. The salinization ratio (Na_2O/K_2O) suggest that Na_2O accumulated here. In addition, leaching ratios suggest that this horizon was poorly leached. The presence of Ni, Cu, and Cr show increases from the presence of clay (detrital) in the Bw 2 horizon. The presence of clays is accompanied by an increase in Al_2O_3. In addition, salinization ($(Na_2O+K_2O)/Al_2O_3$), oxidation, hydrolysis, and calcification all show decreasing trends to further indicate the presence of detrital clays in the B horizons.

KEY

I = Illite
S = Smectite
I/S = mixed-layered
K = Kaolinite
Q = Quartz
C = Calcite

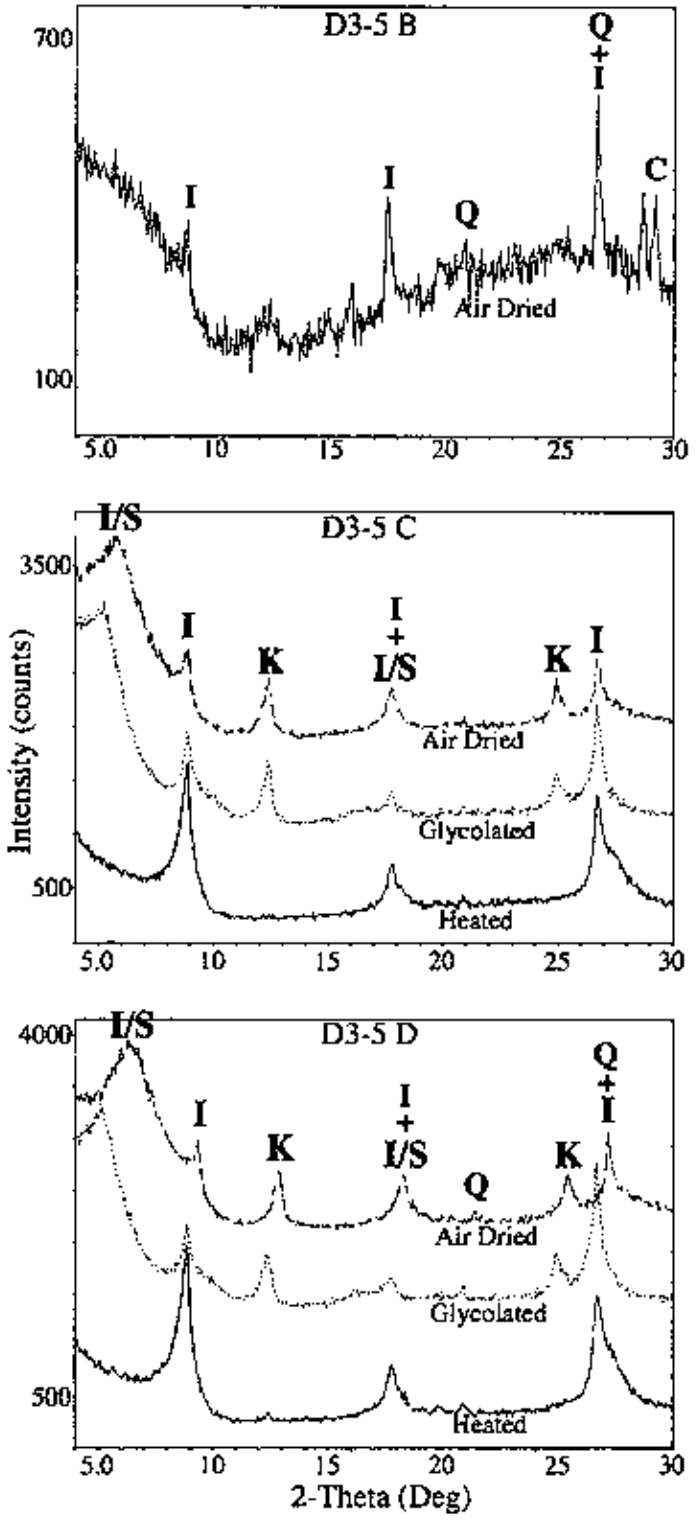

Figure 39. X-ray diffraction of samples D3-5 B-D.

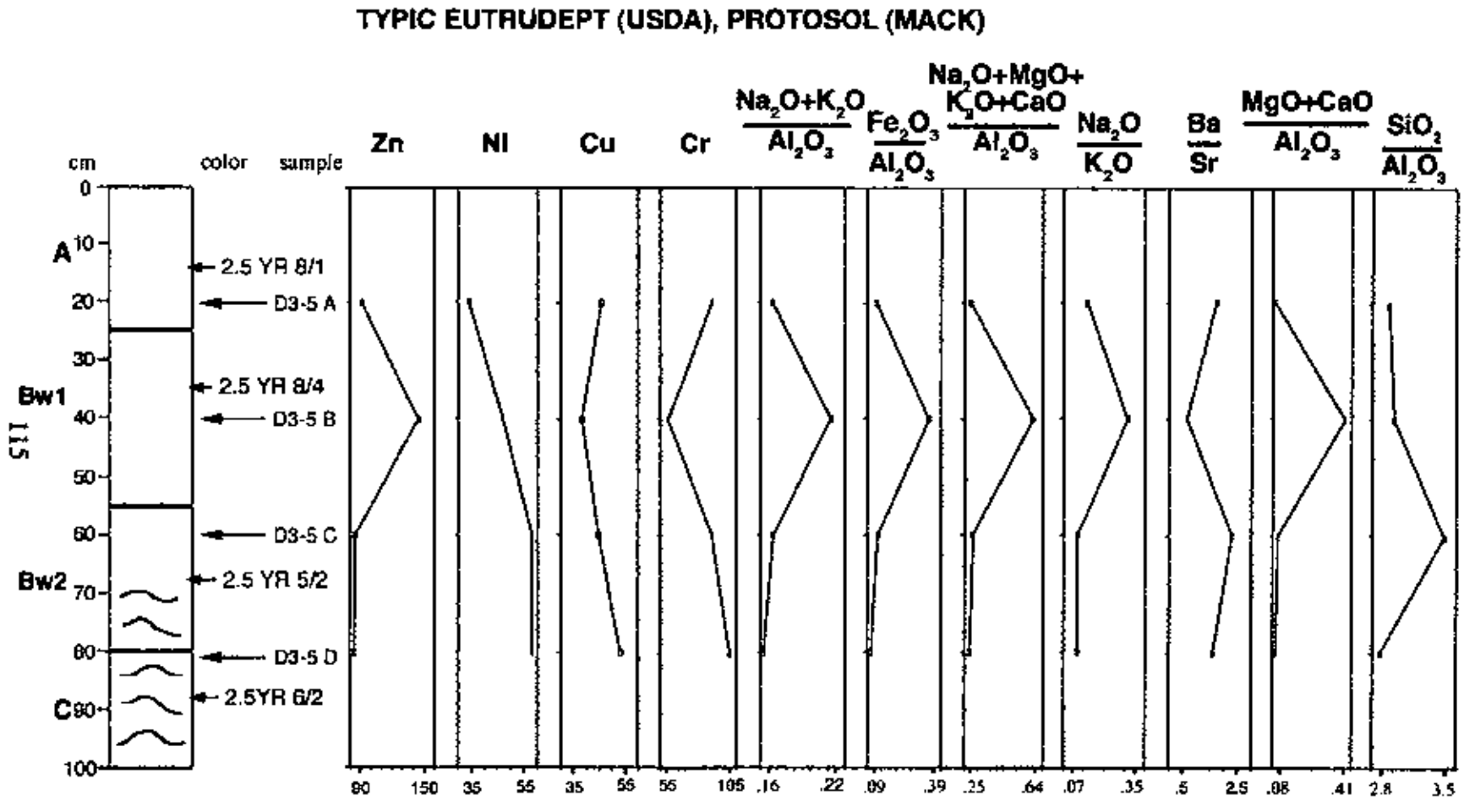

Figure 40. Molecular weathering ratios at Durlston Bay (D3-5).

Classification

I classify this soil using USDA standards as a Typic Eutrudept. The order is interpreted as an Inceptisol and not an Entisol. This is based on the distinctive B horizons in this profile that indicate more development than Entisols. The suborder indicates that development occurred in an udic moisture regime, indicating humid climates that have well distributed rainfall. The great group is based on analysis of molecular weathering ratios that indicate bases accumulated within the profile. The subgroup indicates that there were no other features that could be used to describe this profile.

This soil was classified as a Protosol using the Mack et al. (1993) classification. The order is named for its weak development and its lack of pedogenic features. Subordinate modifiers were not used. I feel that this classification is more descriptive and informative than the USDA classification used above.

SALÈVE (S-19)

Analysis

The S-19 profile at Salève is weakly-developed. Field observations show horizontal infilled burrows in the upper parts of the profile in the A horizon (Table 4). These burrows are interpreted as invertebrate organisms (worms) that eat sediment and leave digestive tracks throughout this horizon. The C1 and C2 horizons display relict bedding. Each horizon is also characterized by color differences. Throughout the profile thin section analysis detected diagenetic minerals, such as hematite, pyrite, and euhedral gypsum (Table 4). XRD analysis indicates the presence of quartz and calcite at the top of

Table 4. Salève paleosol profile (S-19)

Horizon	Description
A	(0-10 cm) Fresh (2.5 YR 7/4 light reddish brown); lime mud; Reacts with HCL; Macro: vertical burrows (wormcasts); Micro: hematite, pyrite, euhedral gypsum, gypsum crystals replaced with pyrite; XRD: quartz, calcite.
C1	(10-20 cm) Fresh (2.5 YR 7/2 pale red); lime mud; Reacts with HCL; Macro: relict bedding; Micro: hematite, pyrite, euhedral gypsum, gypsum crystals replaced with pyrite.
C2	(20-30 cm) Fresh (2.5 YR 8/1 white): lime mud; Reacts with HCL; Macro: relict bedding; Micro: hematite, pyrite, euhedral gypsum, gypsum crystals replaced with pyrite.

the C1 horizon (Figure 36). The molecular weathering ratios show distinct trends throughout the profile (Figure 41). The hydration ratio shows that the presence of clay (detrital) is likely toward the top of the profile in the A horizon. This ratio also shows an area of possible accumulation of clays at the bottom of the profile (at 28 cm). Accumulation of clays (Al_2O_3) in this area is also suggested by the decrease of oxidation. This occurrence of clay at the bottom of the profile might suggest a possible buried soil, perhaps a buried B horizon. The hydrolysis and the calcification ratios do not show a trend or significant change in values. The lower values of the hydration and in the A

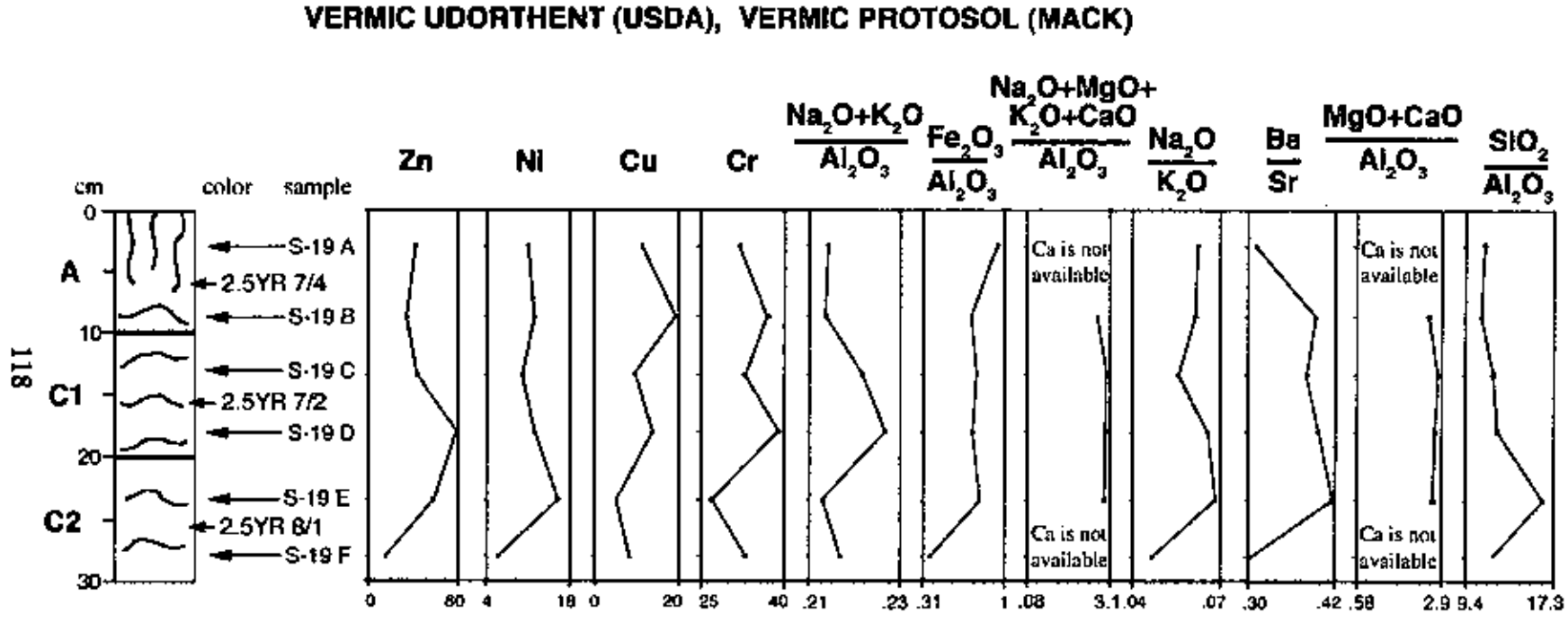

Figure 41. Molecular weathering ratios at Saleve (S-19).

horizon may represent modification from pedogenesis. At the bottom of the C1 and top of the C2 horizon there are increased values in salinization (Na_2O/K_2O). The salinization ratio ($Na_2O+K_2O)/Al_2O_3$) shows an increase at the bottom of the C1 horizon. The trace element Zn shows a significant increase in the C1 and the top part of the C2 horizon. The zig-zag pattern of the trace elements Cu and Cr make these ratios unreliable for interpretation. The leaching ratio also does not agree with other ratios, such as the salinization ratio (Na_2O/K_2O), and cannot be interpreted.

Classification

I classify this soil as a Vermic Udorthent under USDA standards. This name indicates a very weakly developed soil. The taxonomic class is interpreted as an Entisol. The suborder and great group indicate that no other distinguishing characteristics are present. Vermic is used for the subgroup indicating 50% or more of wormholes, wormcasts, and filled animal burrows at a depth no greater than 25 cm.

This paleosol is classified as a Vermic Protosol under Mack et al. (1993) standards. The order is named for its weak development and poorly developed pedogenic features. The most common subordinate modifiers are listed in Mack et al. (1993), and they do not include Vermic. However, this paper (Mack et al., 1993) specifically states that other modifiers can be added if properly defined. Therefore, Vermic is defined and used with the presence of wormholes, wormcasts, and filled animal burrows. I feel that this name describes this soil equally well as the one used above.

CHAPTER 9
CONCLUSION

The lower and upper intervals in the French Jura and the Dorset coast show a distinct Croll-Milankovitch stacking pattern that can be used for regional correlation. The sequences consist of small-scale cycles (PACs) interpreted to be the result of orbitally forced eustatic sea-level changes every 20 ka (6^{th} order cycles). These 20 ka cycles are part of distinctive larger scale sequences that are interpreted to be 3^{th} and 4^{th} order (with periods of 100 ka and 400 ka repectively). Cycles show distinct shallowing upward facies changes and they are bound by distinctive surfaces that mark a change to deeper facies. Distinctive surfaces at most major sequence boundaries (3^{rd} and 4^{th} order) are also unconformable surfaces that mark major flooding events that can be correlated throughout each basin and from the French Jura to the Dorset coast. Distinct surfaces that mark more significant changes in facies can be seen at the boundaries of a 3^{rd} order sequence where the study intervals and formation and member boundaries are present.

The two studied regions (The French Jura and the Dorset coast) show that sections are mostly complete at the type sections in more basinward deposits, whereas deposits closer to the basin margin are more condensed with missing cycles. The type section for the Purbeck (Durlston Bay) is the most complete within the Wessex Basin. The Stair Hole section in England consists of deposits that were located closer to the basin margin and shows 5^{th} and 6^{th} order cycles missing and condensed with 4^{th} order sequences highly condensed. The Paris sub-basin also shows this trend, where the type section (Salève) is the most complete and the other sections are condensed with missing

5th and 6th order cycles. Missing cycles occur throughout all sections near facies that consist of more marl and soil. Cycles show that below 3rd order boundaries facies are more restricted and facies changes within each cycle vary to a lesser degree than that of the cycles just above this boundary. Cycles within both regions are mainly condensed and/or missing at and near major cycle boundaries (3rd and 4th) and are represented by poorly to moderately developed paleosols (Entisols and Inceptisols) or marl and rubble beds. The paleosols on the Dorset coast are more developed than the one's evaluated from the French Jura, and this may suggest that the Dorset coast sections formed closer to the basin margin than the section in the French Jura.

REFERENCES CITED

Allen, P., 1998, Purbeck-Wealden (early Cretaceous) climates: Proceedings of the Geologists Association, v. 109, p. 197-236.

Allen, P, and Wimbledon, W., A. 1991, Correlation of NW European Purbeck-Wealden (nonmarine Lower Cretaceous) as seen from the English type-areas: Cretaceous Research, v. 12, p. 511-526.

Anderson, E.J., Goodwin, P.W. and Sobieski T.H., 1984, Episodic accumulation and the origin of formation boundaries in the Helderberg Group of New York State, Geology, v. 12, p. 120-123.

Anderson, E.J., Goodwin, P.W. and Goodman, P.T., 1986, Reconstruction of patterns of differential subsidence using an episodic stratigraphic model, Spec. Publs. int. Ass. Sediment, v. 8, p. 437-443.

Anderson, E.J, and Goodwin, P.W., 1990, The significance of meter-scale cycles in the quest for a fundamental stratigraphic unit: Journal of the Geological Society, London, v. 147, p. 507-518.

Anderson, E.J., 2000, Cycle Boundaries and the Magnitude and Frequency of Sea-level Rise Events: Examples from the Purbeckian of Dorset. Abstract, IAS-Meeting, Dublin.

Anderson, E.J., 2001a, The Cyclic Structure of the Purbeck Group, Lower Cretaceous Dorset, England. Abstracts, Geol. Soc. Amer., N.E. Section Meeting, Burlington.

Anderson, E.J., 2001b, Asymmetrical Facies patterns in Orbitally Forced 3rd, 4th, 5th and 6th Order Sequences: The Purbeckian of Dorset. Abstracts, SEPM Multidisciplinary Approach to Cyclostratigraphy Workshop, Sorrento.

Anderson, E.J., 2001c, Integration of Bed Descriptions, Molluscan Depth Zones and Faunicycles with an Orbitally Forced Four-tiered Hierarchy of Lithic Allocycles: In the Lower Cretaceous, Purbeckian of Dorset, England. Abstracts, 21st IAS-Meeting, Davos.

Anderson, E.J., 2001d, Lateral Continuity and Discontinuity of 100 ka Eccentricity Sequences within an Orbitally Forced Cyclic Hierarchy: The Purbeck Group, Lower Cretaceous, Dorset, England. Abstracts, Geol. Soc. Amer., Annual Meeting, Boston.

Anderson, F.W., 1985, Ostracod faunas in the Purbeck and Wealden of England: Journal of Micropaleontology, v. 4, p. 1-68.

Berger, A., 1980, The Milankovitch astronomical theory of paleoclimate: a modern review: Vistas in Astronomy, v. 24, pp. 103-122.

Birkland, P.W., 1999, Soils and geomorphology, Oxford, p. 225.

Bulot, L.G., 1995, Les Formations a ammonites du Cretaceous inferieur dans le sud-est de la France (Berriasian a Hauterivien): biostratigraphie, paleontology et cycles sedimentaraires. –These Univ. Grenoble, France, p. 375.

Clements, R.G.,1993, Type-section of the Purbeck Limestone Group, Durlston Bay, Swanage, Dorset: Proceedings of the Dorset Natural History and Archaeological Soc.,114, (for 1992), p.15-41.

Cotillon, P., 1992, Search for eustacy record in deep tethyan deposits through the study of sedimentary flux variations. Application to the Upper Tithonian – Lower Apian series at DSDP Site 534 (central Atlantic). Palaeogeo, Palaeoclim., Palaeoeco., v. 91, p. 263-275.

Croll, J., 1875, Climate and Time in their Geological Relations; a Theory of Secular Changes of the Earth's Climate: Daldy, Ibister & Co., London, p. 577.

Ensom, P.C., 1985, An annoted section of the Purbeck Limestone Formation at Worbarrow Trout, Dorset Proceedings, v. 106, p.87-91.

Feist, M., Lake, R.D., and Wood, C.J., 1995, Charophyte biostratigraphy of the Purbeck and Wealden of southern England: Palaeontology, v. 38, p. 407-442.

Fischer, A.G. and Bottjer, D. J., 1991, Orbital forcing and sedimentary sequences, Journal of Sedimentary Petrology, v. 61, no. 7, p. 1063 – 1069.

Forbes, E., 1851, On the succession of strata and distribution of organic remains in the Dorsetshire Purbecks. Rep. Brit, Assoc. Adv. Sci. (for 1850), p.79-81.

Folk, R.L, 1974, Petrology of sedimentary rocks, Hemphill, Austin, Texas.

Goldhammer, R.K., Dunn, P.A., and haardie, L.A., 1990, Depositional cycles, composite sea-level changes, cycle stacking patterns, and the hierarchy of stratigrphic forcing: Examples from Alpine triassic platform carbonates. Bull. Geol.Soc.Amer., v. 102, p. 535-562.

Goldhammer, R.K, Lehman, p.J., and Dunn, P.A., 1993, The origin of high-frequency platform carbonate cycles and third-order sequences (Lower Ordovician El Paso Gp. West Texas): constraints from outcrop data and stratigraphic modeling. J. sedim. Petrol., v. 63, p. 318-359.

Goodwin, P.W. and Anderson, E. J., 1985, Punctuated Aggradational Cycles: A general hypothesis of episodic stratigraphic accumulation, Journal of Geology, v. 93, p. 515 – 530.

Goodwin, P.W. and Anderson, E.J., 1986, Punctuated Aggradational Cycles: Implications for stratigraphic analysis, Paleoceanography, v. 1, no. 4, p. 417-429.

Goodwin, P.W., and Anderson, E.J., 1988, Episodic development of Helderbergian paleogeography, New York State, Appalachian Basin, *in*, McMillan, N.J., Embry, A.F., and Glass, D.J., eds. Devonian of the World: Second International Symposium on the Devonian System, Canadian Society of Petroleum Geologists, p. 553-568.

Goodwin, P.W., and Anderson, E.J., 1997. Stratigraphic incompleteness: Milankovitch in the Manlius at the margin, *in* Rayne, T.W., Bailey, D.G., and Tewksbury, B.J., eds., Field Trip Guide for the 69th Annual Meeting of the New York State Geological Association, p. 237-249.

Gradstein, F.M., Agterberg, F.P., Ogg, J.G, Hardenbol, J., van Veen, P., Thierry, J. and Huang, Z., 1994, A Mesozoic time scale, Journal of Geophysical Research, v. 99, p. 24051-24074.

Gradstein, F.M., Agterberg, F.P., Ogg, J.G, Hardenbol, J., van Veen, P., Thierry, J. and Huang, Z., 1995, A Triassic, Jurassic and Cretaceous time scale. In: Geochonology, Time Scales and Global Stratigraphic Correlation (Ed. By W. A. Berggren, D.V. Kent, M.P. Aubry and J. Hardenbol), SEPM, no. 54, p. 95-126.

Häfeli, C.,1966, Die Jura/Kreide-grenzgeschichte im Bielerseegebeit (Kt Bern), Eclogae geol. Helv., no. 59, v.2, p. 565-695

Hillgärtner, H., 1998, Discontinuity surfaces on a shallow-marine carbonate platform (Berriasian, Valanginian, France, And Switzerland): Journal of Sedimentary Research, v. 68, no. 6, p. 1093 – 1108.

Hillgärtner, H., 1999, The evolution of the French Jura platform during the Late Berriasian to Early Valanginian: controlling factors and timing: Institute de Geologie de L'Universite de Fribourg (Suisse), Multiprint SA, Fribourg, These n 1240.

Horne, D.J., 1995, A revised ostracod biostratigraphy for the Purbeck-Wealden of England: Cretaceous Research, v. 16, p. 639-663.

House, R.M., 1985, A new approach to an absolute timescale from measurements of orbital cycles and sedimentary microrhythms, Nature, v. 315, no. 27, p. 721-725.

House, R.M., 1995, orbital forcing timescales: an introduction, from House, M.R. and Gale, A.S. (eds), 1995, Orbital Forcing and Cyclostratigraphy, Geological Society Special Publication, no. 85, p. 1-18.

Jacquin, T., Rusciadelli, G., De Graciansky, P., and Magniez-Jannin, F., 1998, The North Atlantic cycle: an overview of 2nd-order transgressive/regressive facies cycles in the Lower Cretaceous of Western Europe, in, De graciansky, P., Hardenbol, J., Jacquin, T., and Vail, P.R., eds, Mesozoic and Cenozoic Sequence Stratigraphy of European Basins: SEPM Special Publication, no. 60, p. 397-409.

Le Hegarat, G., 1980, Berriasisan. – in Cavelier, J. & Roger, J (eds): Les etages francais et leurs stratotypes, Mem. Bur. Rech. Geol. Min., v. 109, p. 567.

Mack, Greg, H., James, Calvin W., Monger, Curtis H.,1993, Classification of Paleosols. Geological Society of America Bulletin, v. 105, p. 129-136.

Marbut, C. F., 1935, Atlas of American culture. Part III. Soils of the United States. Washington: Government Printer.

Milankovitch, M., 1941, Kanon der erdbestrahlung and sein anwendung auf des eiszeitenproglen. Academic Royale Serbe, Belgrade, special edition, v. 133, p. 633.

Montiel, E., 1993, Some important upper Tithonian and Berriasian dinoflagellate cysts of SE France: integrated biostratigraphy and sequence stratigraphy, Bull. Cent. Rech.-Expl. Elf-Aquitaine, Pau-SNPA, v. 17, p. 249-273.

Moore, D.M, and Reynolds, R.C., Jr., 1997, X-ray diffraction and the identification and analysis of clay minerals, Oxford University Press, pp. 332.

Morter, A.A., 1984, Purbeck-Wealden Beds Mollusca and their relationship to ostracod biostratigraphy, stratigraphical correlation and paleoecology in the Weald and adjacent areas, Proc. Geol. Assoc., v. 95, pp 217-234.

Munsell Color, 1975, Munsell Soil Color Charts: Baltimore, Munsell Color Company, p. 24.

Olsen, P.E., 1986, A 40-million year lake record of early Mesozoic orbital forcing. Science, v. 234, p. 842-848.

Pasquier, J-B. and Strasser, A., 1997, Platform-to–basin correlation by high-resolution sequence stratigraphy and cyclostratigraphy (Poster), Session No. 18 booth# 16.

Retallack, G.J., 1983, Late Eocene and Oligocene Paleosols from Badlands National Park, South Dakota: Geological Society of America Special Paper193, p. 82.

Retallack , G.J., 1990, Soils of the past: an introduction to paleopedology. Allen & Unwin, London, p. 520.

Retallack, G.J.,1997, A color guide to paleosols: John Wiley & Sons, New York, p. 43-60.

Ruffel, A., 1991, Sea-level events during the Early Cretaceous in Western Europe, Cretaceous Research, vol. 12, p. 527-551.

Soil Survey Staff, 1998, Keys to soil Taxonomy: U.S. Department of Agriculture, Eighth Edition, p. 327.

Seier and Anderson, 2002, Cyclic stratigraphy and facies change across a 3rd order boundary (Upper berriasian) Lower Cretaceous in the French Jura and Dorset, England. Geol. Soc. Amer., N.E. Section Meeting, Abstract, v. 34, no. 1, March, Springfield, Mass.,

Strasser, A.,1988, Shallowing-upward sequences in the Purbeckian peritidal carbonates (lowermost Cretaceous, Swiss and French Jura Mountains), Sedimentology, v. 35, p. 369-383.

Strasser, A., 1994, Milankovitch cyclicity and high-resolution sequence stratigraphy in Lagoonal-peritidal carbonates (Upper Tithonian-Lower Berriasian, French Jura Mountains), in De Boer, P.L. & Smith, D.G. (eds.), Orbital forcing and cyclic sequences.- International Assoc. Sed., Spec.Pub, v. 19, p. 285 – 301.

Strasser, A, and Hillgärtner, H., 1998, high-frequency sea-level fluctuations recorded on a shallow carbonate platform (Berriasian and Lower Valanginian of Mount Salève, French Jura): Eclogae geol., v. 91, p. 375-390.

Strasser, A., Pittet, B., Hillgärtner, H., Pasquier, J-B., 1999, Depositional sequences in shallow carbonate-dominated sedimentary systems: concepts for a high-resolution analysis, v.128, p. 201-221.

Vail, P.R., Mitchum, R.M., and Thompson, S. III, 1977, Seismic stratigraphy and global change of sea-level, Part3: relative changes of sea-level from coastal onlap. In Payton, C.W. ed., Seismic stratigraphic applications to hydrocarbon exploration, American Association of Petroleum geologist Memoir, v. 26, p. 63-97.

Van Wagoner, J.C., Posamentier, H.W., Mitchum, R.M., Vail, P.R., Sarg, J.F., Loutit, T.S., and Hardenbol, J., 1988, An overview of the fundamentals of sequence stratigraphy and key definitions. in Wilgus, C.K., Hastings, B.J., and Posamentier, H.W., and Van Wagoner, J.C. eds, Sea-level change an integrated approach. SEPM Special Publication, v. 42, p. 39-46.

Weasthead, R.K. and Mather, A.E., 1996, An updated lithostratigraphy for the Purbeck Limestone Group in the Dorset type-area, Proceeding of the Geologists Association, v.107, p. 117-128.

Wimbledon, W.A. and Cope, J.C, 1978, The ammonite faunas of the English Portland beds and the zones of the Portlandian Stage, J. geol. Soc. London, v. 135, p. 183-190.

Wimbledon, W.A. and Hunt, C.O., 1983, The Portland-Purbeck junction (Portlandian-Berriasian) in the Weald, and correlation of latest Jurassic-early Cretaceous rocks in southern England, Geolog. Mag., v. 120, no. 3, p. 267-280.

Wimbledon, W.A., 1987, Rhythmic sedimentation in the Late Jurassic-Early Cretaceous, Rythmic Sedimentation, p. 127-133.

Wright, V.P., 1994, Paleosols in shallow marine carbonate sequence. Earth-Science Reviews. No. 35, p. 367-395.

Wright, V.P., 1996, Use of paleosols in sequence stratigraphy of peritidal carbonates. Geological Society Special Publication, no. 103, p. 63-74.

APPENDIX A : THIN SECTION ANALYSIS

NO.	FOLK (1974) CLASSIFICATION	OTHER OBSERVATIONS
upper	Saleve	
S-1	sparse biomicrite	foraminifera, calpionellids, pelecypods, peloids, geopetal structures, intraclasts, stylolites
S-3	packed biomicrite	foraminifera, calpionellids, pelecypods, ostracods, gastropods, peloids, intraclasts, iron oxides, iron sulfides, Dasycladacean green algae, geopetal structures
S-4	poorly washed sparite	foraminifera, pelecypods with microstalactitic cement, ostracods, geopetal structures, intraclasts
S-5	packed biomicrite	foraminifera, calpionellids, pelecypods, ostracods, gastropods, peloids, Dasycladacean green algae
S-6	packed biomicrite	foraminifera, calpionellids, pelecypods, ostracods, intraclasts, stylolites
S-7	poorly washed intrasparite	foraminifera, pelecypods with microstalactitic cement, peloids, Dasycladacean green algae
S-8	packed biomicrite	foraminifera, calpionellids, pelecypods, ooids, Dasycladacean green algae
S-9	sparse biomicrite	foraminifera, ostracods, gastropods
S-10	packed intramicrite	foraminifera, calpionellids, intraclasts, peloids, ooids
S-11	poorly washed biopelsparite	foraminifera, pelecypods with microstalactitic cement, ostracods, Intraclasts, peloids
S-12	poorly washed biopelsparite	foraminifera, calpionellids, pelecypods, ostracods, intraclasts, peloids
S-14	packed biomicrite	foraminifera, calpionellids, pelecypods, ostracods
S-15	packed biomicrite	foraminifera, pelecypods with microstalactitic cement, ostracods, intraclasts
S-16	packed biomicrite	foraminifera, pelecypods, ostracods
S-17	packed biomicrite	foraminifera, calpionellids, pelecypods, vegetative part of a charophyte
S-18	packed biomicrite	foraminifera, Dasycladacean green algae, vegetative part of a charophyte
S-19 A	*Paleosol	hematite, pyrite, euhedral gypsum, quartz gypsum crystals replaced with pyrite, quartz
S-19 B	*Paleosol	hematite, pyrite, euhedral gypsum, quartz gypsum crystals replaced with pyrite, quartz
S-19 C	*Paleosol	hematite, pyrite, euhedral gypsum, quartz gypsum crystals replaced with pyrite, quartz
S-19 D	*Paleosol	hematite, pyrite, euhedral gypsum, gypsum crystals, quartz
S-19 E	*Paleosol	less iron, hematite, pyrite, euhedral gypsum, quartz gypsum crystals replaced with pyrite
S-20	pelmicrite	
S-22	packed biopelmicrite	intraclasts, ooid, enchinoderm spines, pelecypods with microstalactitic cement
S-23	packed biopelmicrite	foraminifera, pelecypods, enchinoderm spines, intraclasts

* Folk (1974) classification does not apply.

APPENDIX A (continued)

Upper	Chapeau de Gendarme	
G-1	unsorted biopelsparite	foraminifera, pelecypods, intraclasts
G-2	poorly washed biosparite	foraminifera, calpionellids, ostracods, intraclasts, peloids, pelecypods with microstalactitic cement
G-3	packed biopelmicrite	foraminifera, pelecypods, intraclasts, peloids, pelecypods with microstalactitic cement
lower	Crozet	
R-0	fossiliferous micrite	foraminifera, pelecypods, ostracods
R-1	fossiliferous micrite	foraminifera, pelecypods, ostracods
R-2 A	*Paleosol	black organic peat, plant fragments
R-2 B	*Paleosol	
R-2 C	*Paleosol	foraminifera, little iron, hematite, pyrite, quartz, fine grained dolomite
R-2 D	*Paleosol	little iron, hematite, pyrite, quartz, fine grained dolomite
R-2 E	*Paleosol	more iron, hematite, pyrite, quartz, fine grained dolomite
R-3	fossiliferous micrite	foraminifera, pelecypods, ostracods
R-3.1	micrite	foraminifera
R-3.2	micrite	
R3.3	micrite	
R-4	micrite	
R-5	micrite	patches of packed biomicrite, foraminifera, pelecypods, intraclasts, peloids
R-6	micrite	laminated
R-7	micrite	
upper	Crozet	
C-1	packed biomicrite	foraminifera, pelecypods, ostracods, gastropods, peloids
C-3	poorly washed biosparite	foraminifera, pelecypods, gastropods, peloids
C-4	packed biopelmicrite	foraminifera, pelecypods, gastropods, peloids
C-5	poorly washed intrapelsparite	foraminifera, peloids
C-6	poorly washed intrasparite	foraminifera, pelecypods
C-7	packed biomicrite	foraminifera, pelecypods, ostracods, calpionellids
C-8	packed biopelmicrite	pelecypods, ostracods, calpionellids, gastropods, intraclasts
C-9	packed biomicrite	pelecypods, ostracods, foraminifera
C-11	unsorted pelsparite	pelecypods, foraminifera, possible plant roots?
lower	Stair Hole	
H-1	packed biomicrite	pelecypods
H-3	micrite	
H-4	micrite	
H-5	micrite	
upper	Stair Hole	
S-1	unsorted biosparite	pelecypods
S-2	unsorted biosparite	pelecypods

APPENDIX A (continued)

S-3	Sparse biomicrite	pelecypods
S-4	micrite	pelecypods, peloids
S-4	unsorted biosparite	pelecypods, peloids
S-5	micrite	pelecypods
S-6	packed biomicrite	pelecypods, peloids
S-6	pelmicrite	
lower	Durleton Bay (South)	
D1-1 A	*Paleosol	clay, quartz, plant fragments (cellular structure), dolomite, hematite, pyrite
D1-1 B	*Paleosol	clay, quartz, plant fragments (cellular structure), dolomite, hematite, pyrite
D1-1 C	*Paleosol	clay, quartz, plant fragments (cellular structure), dolomite, hematite, pyrite
D1-1 D	*Paleosol	clay, quartz, plant fragments (cellular structure), dolomite, hematite, pyrite
D1-4	unsorted biosparite	pelecypods, blackened pelecypods
upper	Durleton Bay (North)	
D3-6	poorly washed biosparite	pelecypods, blackened pelecypods
D3-7	unsorted biosparite	pelecypods
D3-8	unsorted biosparite	pelecypods, blackened pelecypods
D3-5 A	*Paleosol	euhedral gypsum, clay, clumps of green clay, quartz, plant fragments, dolomite, shells
D3-5 B	*Paleosol	
D3-5 C	*Paleosol	euhedral gypsum, clay, quartz, plant fragments, dolomite, shells, more iron, hematite, pyrite
D3-5 D	*Paleosol	euhedral gypsum, clay, quartz, plant fragments, dolomite, shells, hematite, pyrite

APPENDIX II
MICROFACIES

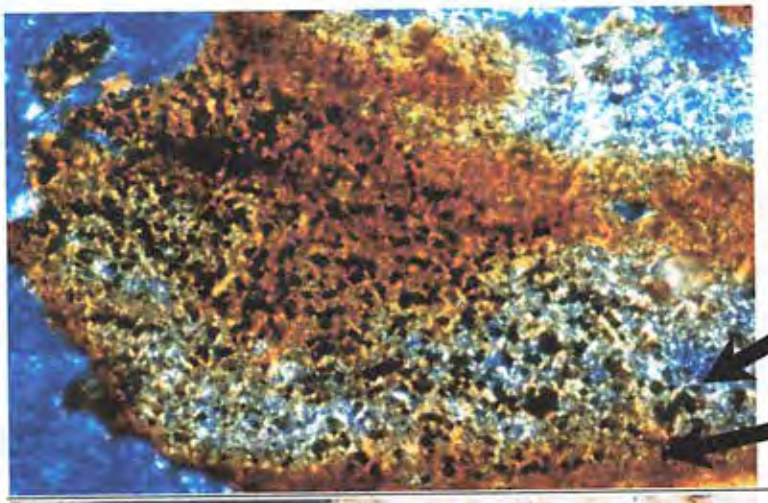

Sample D3-5 D, 20x, Paleosol.

A cluster of diagenetic iron, with possible organics.

Goethite or organic material.

Hematite.

50μm ■

Sample D3-5 C, 20x, Paleosol.

Pelecypods infilled with diagenetic iron and possible organics. The same slide is shown below in reflected light to show traces of pyrite.

50μm ■

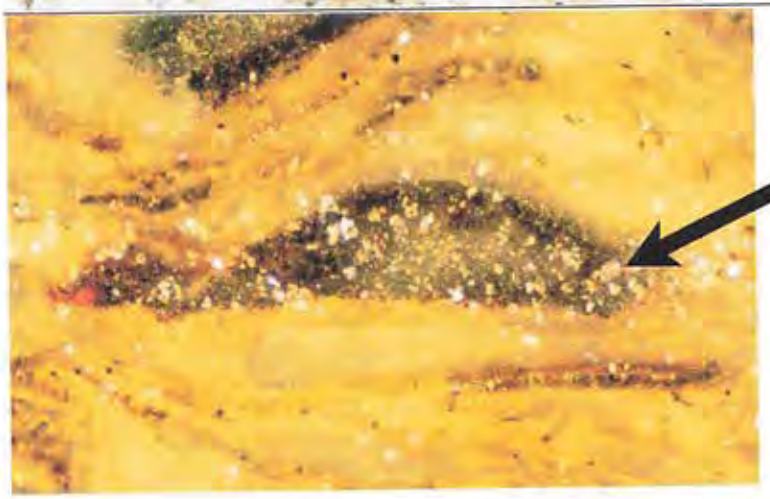

Sample D3-5 C, 20x, reflected light, Paleosol.

The same infilled pelecypod shell as above showing pyrite.

50μm ■

APPENDIX B
(continued)

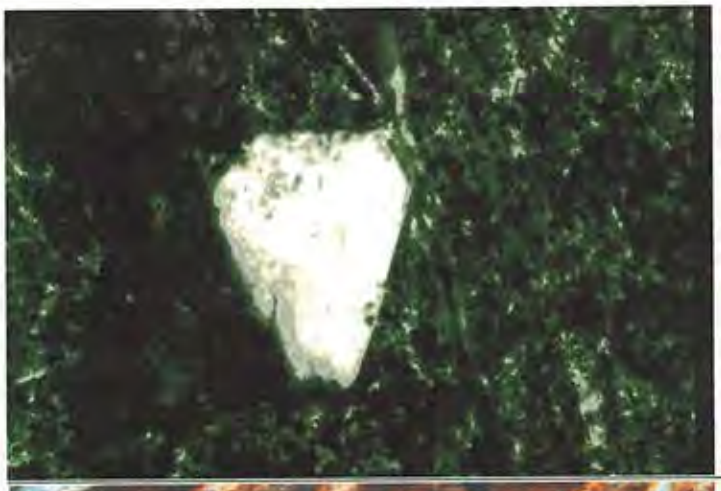

Sample D3-5 A, 20x, Paleosol.

Euhedral gypsum that is diagenetic in origin. The edges show alteration to clay.

100μm ▬

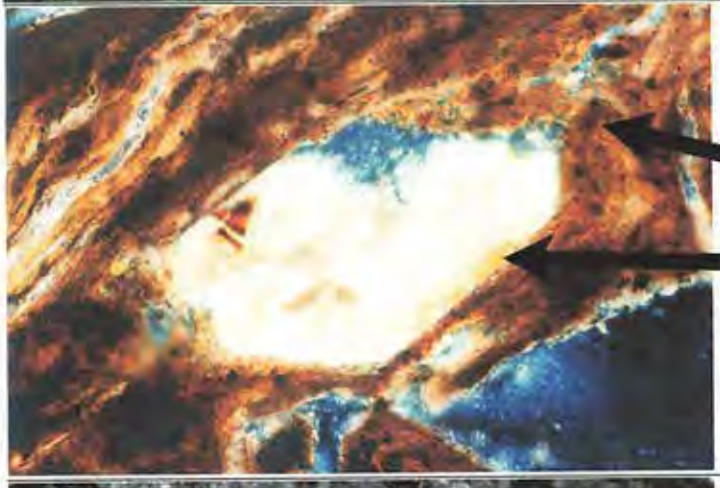

Sample D3-5 C, 10x, Paleosol.

Clay.

Euhedral gypsum that is diagenetic in origin. The edges show alteration to clay.

100μm ▬

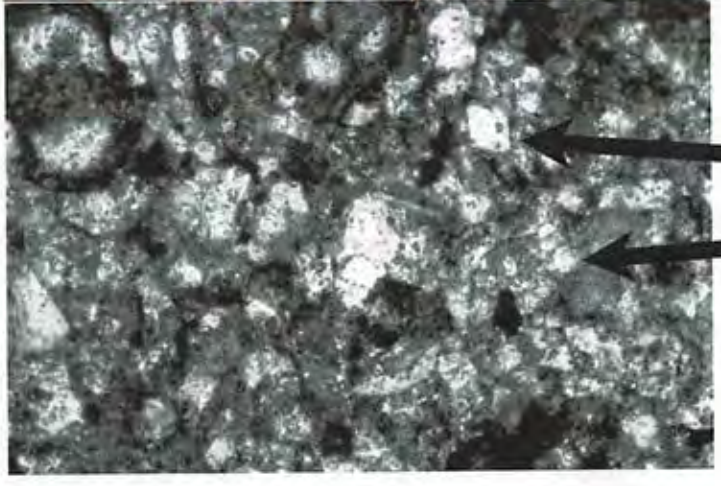

Sample R-2 B, 20x, Paleosol.

Euhedral gypsum.

This slide shows an abundance of quartz.

100μm ▬

APPENDIX B
(continued)

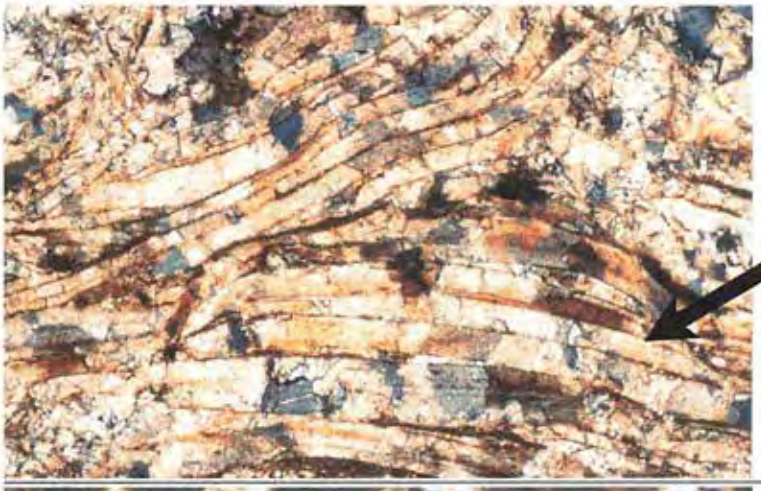

Sample S-1, 10x, Sparse biomicrite.

Pelecypod shells showing original texture with parallel fiberous structures running sub-parallel.

100μm

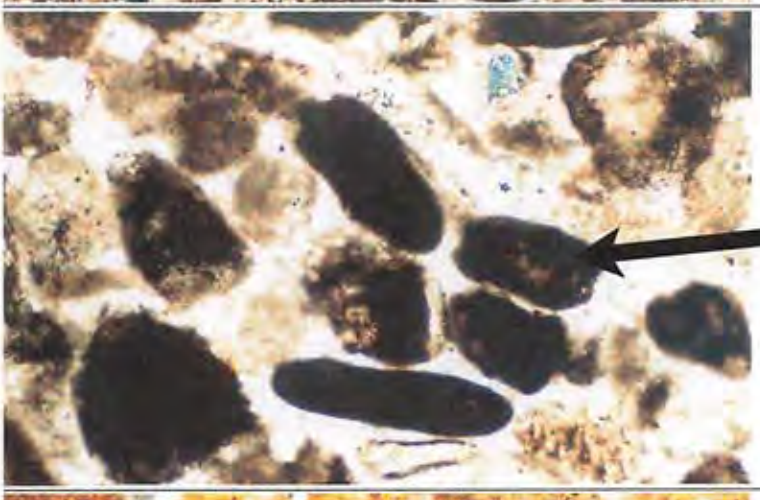

Sample C-11, 20x, Unsorted pelsparite.

Black peloids replacd with ferric iron (Goethite).

50μm

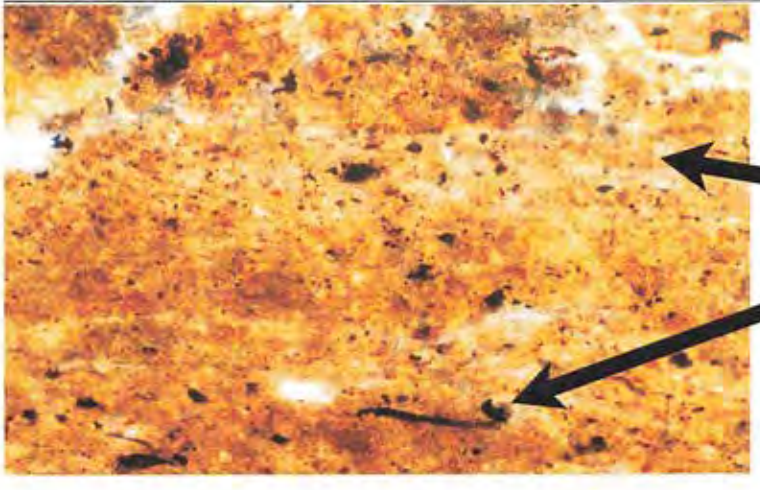

Sample D3-5 C, 10x, Paleosol.

Clay

Detrial plant fragments and organic material.

100μm

APPENDIX B
(continued)

Sample S-15, 20x, Packed biomicrite.

A miliolid foram with the walls filled with micrite and the pores filled with calcite spar.

100μm ▬

Sample S-8, 4x, Packed biomicrite.

A miliolid foram with the walls filled with micrite and the pores filled with calcite spar.

175μm ▬

Sample S-18, 10x, Packed biomicrite.

Gastropod with the walls filled with micrite and the pores filled with calcite spar.

A miliolid foram.

25μm ▬

APPENDIX B
(continued)

Sample R-3.2, 10x, Micrite.

100μm ▬

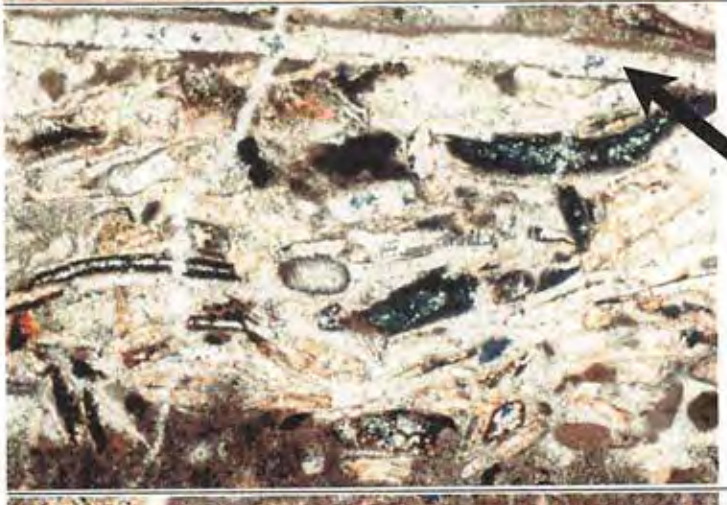

Sample S-1 at Stair Hole, 4x, Unsorted biosparite.

Pelecypod shell replaced with calcite spar.

1000μm ▬

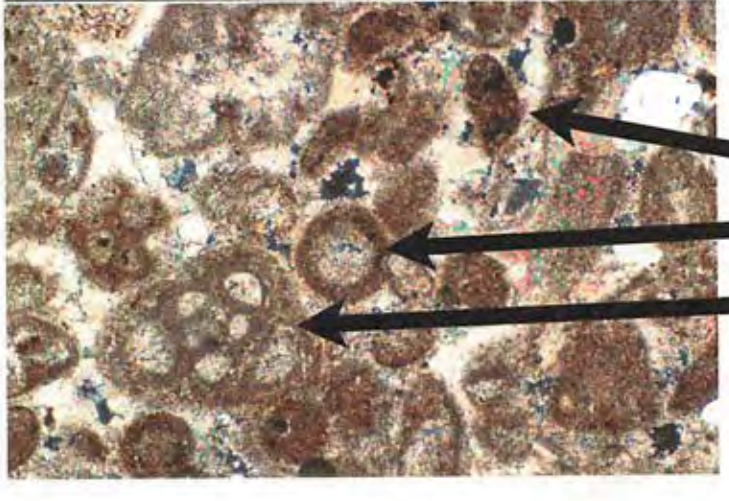

Sample S-11, 10x, Poorly washed biopelsparite.

Black peliods.

Possible brachiopod spine.

Miliolid foram.

100μm ▬

APPENDIX B
(continued)

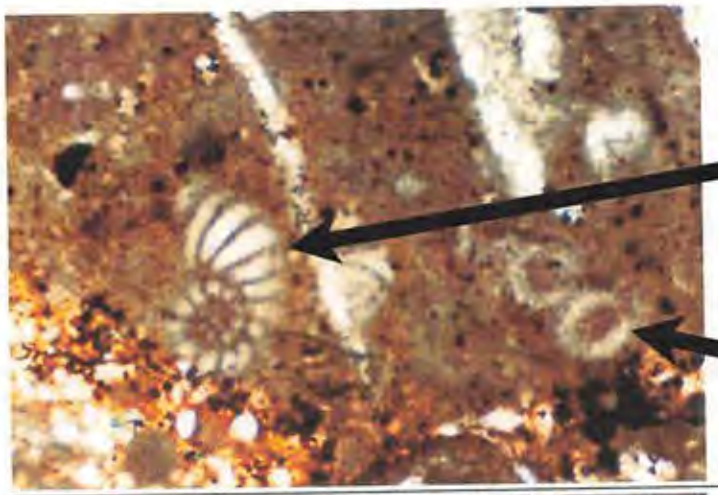

Sample S-14, 10x, Packed biomicrite.

Peneroplid foram with the walls filled with micrite and hematite, and the pores filled with calcite spar.

Possible gastropod.

100μm ■

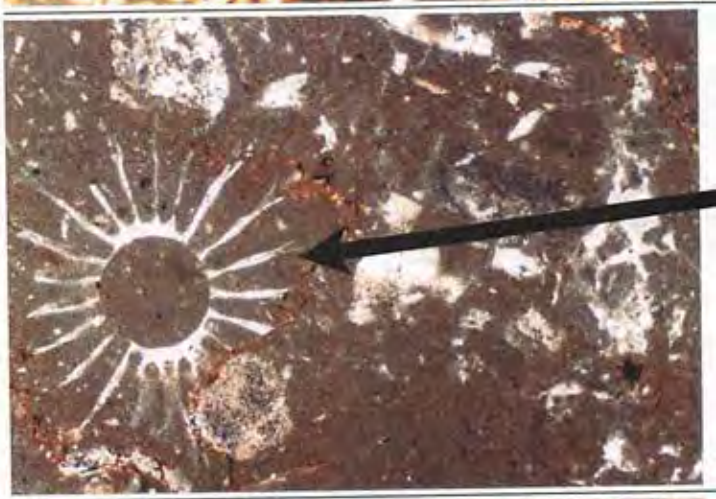

Sample S-8, 4x, Packed biomicrite.

Cross section of a poorly preserved Dasycladacean green algae.

1000μm ■

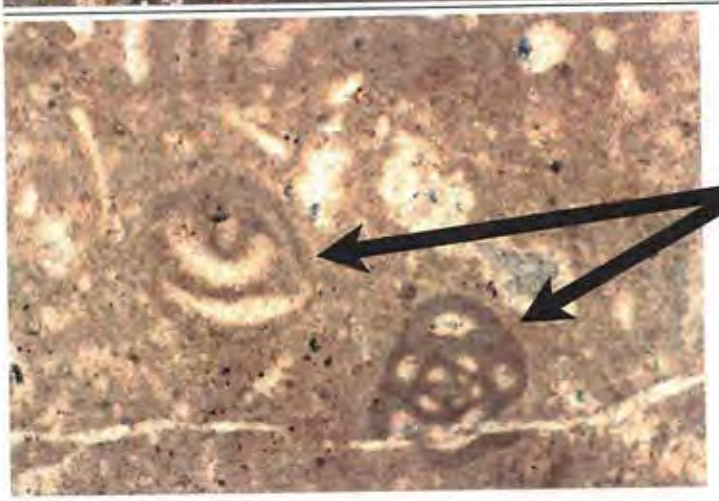

Sample S-18, 10x, Packed biomicrite.

Two Miliolid forams with the walls replaced with micrite and the pores filled with calcite spar.

100μm ■

APPENDIX B
(continued)

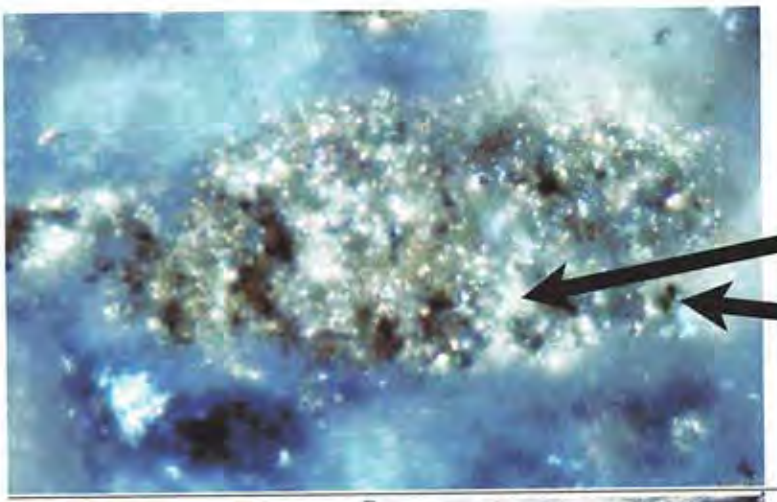

Sample C-11, 40x, reflected light, Unsorted pelsparite.

Diagenetic pyrite.

Goethite

25μm

Sample D-3, 10x, reflected light, Poorly washed biosparite.

This slide shows pelecypod shells that have been replaced with ferric iron (geothite), with little pyrite.

80μm

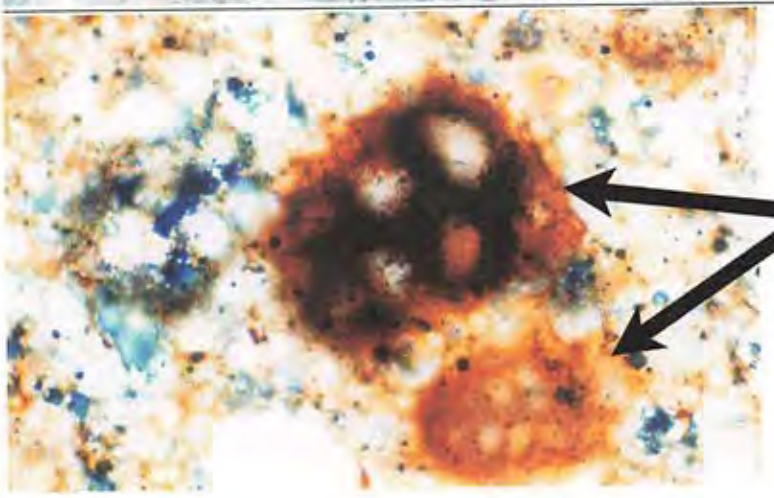

Sample D3-5 C, 10x, Paleosol.

Two miliolid forams with their walls stained with ferric iron (goethite) and hematite (reddish orange). The pores are filled with calcite spar.

100μm

APPENDIX C
ICP-MS DATA

RAW DATA FROM ICP ANALYSIS: units are in grams per 100 grams of sample or ppm

cm		Na	Mg	Al	K	Ca	Fe	Si	ppm Zn	ppm Ni	ppm Cu	ppm Cr	ppm Ba	ppm Sr
	Durlston Bay (North)													
90	D1-6A	0.16	1.89	8.37	3.21	1.56	3.65	22.1	41.2	39	23.1	92	204	144
80	D1-6B	0.14	1.79	8.5	3.09	1.61	3.38	24.7	42.1	44	33.3	91	181	126
60	D1-6C	0.14	1.44	5.83	2.11	12.5	2.42	16.9	68.5	39	31.5	65	192	529
10	D1-6D	0.12	1.22	4.34	1.62	*	1.88	13.1	22.7	29	39.2	48	118	448
	Durlston Bay (South)													
20	D3-5A	0.28	0.8	9.76	2.39	1.44	3.99	25.9	90.8	34	45.9	91	280	161
40	D3-5B	0.5	0.48	6.03	1.57	6.2	6.97	16.7	145	47	38.3	56	176	264
60	D3-5C	0.15	0.76	8.67	2.23	1.47	2.6	27.2	84.9	58	44.4	91	352	152
81	D3-5D	0.17	0.9	10.3	2.55	1.33	2.9	26.2	83.7	58	53.2	105	283	177
	Crozet													
9	R-2A	0	0.08	0.42	0.13	3.21	11.5	1.1	20.2	57	13.4	24	47	33.4
40	R-2B	0.03	0.45	0.67	0.3	*	0.54	2.1	6.8	9	15.9	3	19	395
60	R-2C	0.03	0.48	1.02	0.5	*	0.53	4.1	7.5	8	13.3	4	30	376
90	R-2D	0.03	0.51	1.08	0.47	*	0.47	3.3	8	9	19.1	13	26	495
130	R-2E	0.04	0.54	1.13	0.52	*	0.67	3.8	10.1	13	15.8	5	30	482
	Saleve													
3	S-19A	0.04	2.97	2.01	0.64	*	1.88	17	41.6	11	11.3	32	57	183
9	S-19B	0.05	3.57	2.55	0.81	13.6	1.72	21.3	33.2	12	19.2	37	63	160
12	S-19C	0.04	3.51	2.15	0.72	12.9	1.57	19.6	43.1	10	9.6	33	56	147
18	S-19D	0.05	3.91	2.23	0.76	12.5	1.53	25.3	79.6	12	13.8	39	60	151
23	S-19E	0.03	2.48	1.4	0.44	7.49	1.06	21.5	58.4	16	5.2	27	37	88.1
27	S-19F	0.03	2.59	1.95	0.64	*	0.52	19.5	14.5	6	8.2	33	50	165

* = over detection limit.

APPENDIX C
(continued)

Weight percent of oxide

	Na2O	MgO	Al2O3	K2O	CaO	FeO	SiO2
D1-6A	0.22	3.13	15.82	3.87	2.18	4.7	47.26
D1-6B	0.19	2.97	16.06	3.72	2.25	4.35	52.74
D1-6C	0.19	2.39	11.02	2.54	17.49	3.11	36.09
D1-6D	0.16	2.02	8.2	1.95	*	2.42	28.07
D3-5A	0.38	1.33	18.44	2.88	2.01	5.13	55.37
D3-5B	0.67	0.8	11.39	1.89	8.68	8.97	35.62
D3-5C	0.2	1.26	16.38	2.69	2.06	3.34	58.08
D3-5D	0.23	1.49	19.46	3.07	1.86	3.73	56.07
R-2A	0	0.13	0.79	0.16	4.49	14.79	2.37
R-2B	0.04	0.75	1.27	0.36	*	0.69	4.49
R-2C	0.04	0.8	1.93	0.6	*	0.68	8.69
R-2D	0.04	0.85	2.04	0.57	*	0.6	7.04
R-2E	0.05	0.9	2.14	0.63	*	0.86	8.04
S-19A	0.05	4.93	3.8	0.77	*	2.42	36.26
S-19B	0.07	5.92	4.82	0.98	19.03	2.21	45.53
S-19C	0.05	5.82	4.06	0.87	18.05	2.02	41.85
S-19D	0.07	6.48	4.21	0.92	17.49	1.97	54.02
S-19E	0.04	4.11	2.65	0.53	10.48	1.36	45.95
S-19F	0.04	4.29	3.68	0.77	*	0.67	41.8

APPENDIX C
(continued)

	Hydrolysis	leaching	salinization	Oxidation	Hydration	Calcification	Na/K
D1-6A	0.59	1.42	0.26	0.3	2.99	0.34	0.06
D1-6B	0.57	1.44	0.24	0.27	3.28	0.33	0.05
D1-6C	2.05	0.36	0.25	0.28	3.28	1.8	0.07
D1-6D	*	0.26	0.26	0.29	3.42	*	0.08
D3-5A	0.36	1.74	0.18	0.28	3	0.18	0.13
D3-5B	1.06	0.67	0.23	0.79	3.13	0.83	0.36
D3-5C	0.38	2.32	0.18	0.2	3.55	0.2	0.08
D3-5D	0.34	1.6	0.17	0.19	2.88	0.17	0.07
R-2A	6.02	1.41	0.2	18.64	2.99	5.83	0
R-2B	*	0.05	0.32	0.55	3.55	*	0.11
R-2C	*	0.08	0.33	0.35	4.51	*	0.07
R-2D	*	0.05	0.3	0.3	3.45	*	0.07
R-2E	*	0.06	0.32	0.4	3.77	*	0.09
S-19A	*	0.31	0.22	0.64	9.55	*	0.07
S-19B	5.39	0.39	0.22	0.46	9.45	5.18	0.07
S-19C	6.1	0.38	0.23	0.5	10.3	5.88	0.06
S-19D	5.92	0.4	0.23	0.47	12.82	5.69	0.07
S-19E	5.73	0.42	0.22	0.52	17.37	5.52	0.08
S-19F	1.39	0.3	0.22	0.18	11.35	*	0.05